

# Vine copula mixture models and clustering for non-Gaussian data

Özge Sahin<sup>a,\*</sup>, Claudia Czado<sup>a</sup>

<sup>a</sup>*Department of Mathematics, Technische Universität München, Boltzmanstraße 3, 85748 Garching, Germany*

---

## Abstract

The majority of finite mixture models suffer from not allowing asymmetric tail dependencies within components and not capturing non-elliptical clusters in clustering applications. Since vine copulas are very flexible in capturing these types of dependencies, we propose a novel vine copula mixture model for continuous data. We discuss the model selection and parameter estimation problems and further formulate a new model-based clustering algorithm. The use of vine copulas in clustering allows for a range of shapes and dependency structures for the clusters. Our simulation experiments illustrate a significant gain in clustering accuracy when notably asymmetric tail dependencies or/and non-Gaussian margins within the components exist. The analysis of real data sets accompanies the proposed method. We show that the model-based clustering algorithm with vine copula mixture models outperforms the other model-based clustering techniques, especially for the non-Gaussian multivariate data.

*Keywords:* Clustering, copula, dependence, mixture model, non-Gaussian, vine copula

---

## 1. Introduction

Finite mixture models are convenient and statistical tools for model-based clustering. In this framework, one assumes that observations in the multivariate data can be clustered using  $k$  components. Each component has its density, and each observation is assigned to a component with a probability. The book of McLachlan & Peel (2000) provides more details about the finite mixture models. Both Bouveyron & Brunet-Saumard (2014) and McNicholas (2016) review recent model-based clustering methods.

One of the main questions to be addressed in the finite mixture models is *how to select the density of each component*. An early answer to this question is to assume a symmetric distribution such as multivariate Gaussian distribution (e.g., Celeux & Govaert (1995); Fraley & Raftery (1998)) or multivariate t distribution (e.g., Peel & McLachlan (2000); Andrews & McNicholas (2011)). However, these models cannot accommodate the shape of asymmetric components. Hennig (2010) showed one such data example. Their skewed formulations, therefore, have been extensively studied (e.g., Lin et al. (2007); Lee & McLachlan (2014)).

Additionally, the models based on other distributions, for example, shifted asymmetric Laplace distributions (Franczak et al. (2014)), multivariate power exponential distributions (Dang et al. (2015)), and generalized hyperbolic distributions (Browne & McNicholas (2015)) have been proposed for the past few years. Since one of the main interests of copulas is to relax the normality assumption both in marginal distributions and dependence structure, the finite mixture models with copulas have also been studied (e.g., Diday & Vrac (2005); Kosmidis & Karlis (2016)). Cuvelier & Fraiture (2005) worked with the Clayton copula to represent lower tail dependence within the components, while Vrac et al. (2005) applied the Frank copula to have non-Gaussian but symmetric dependence. Nevertheless, these methods raise another question in the finite mixture models: *how to select flexible densities of each component* so the model can represent different asymmetric or/and tail dependencies for different pairs of variables. For this question, the vine

---

\*Corresponding author

*Email addresses:* [ozge.sahin@tum.de](mailto:ozge.sahin@tum.de) (Özge Sahin), [cczado@ma.tum.de](mailto:cczado@ma.tum.de) (Claudia Czado)

copula or pair copula construction is a flexible and efficient tool in high-dimensional dependence modeling (Joe (1996), Aas et al. (2009)).

Applying the vine copula in finite mixture models has been explored before (e.g., Kim et al. (2013); Sun et al. (2017)). However, they only worked with a subclass of vine tree structures and a small number of pair copula families. Therefore, a vine copula mixture model with all classes of vine tree structures and many different pair copula families is needed. Since it provides flexible densities, formulating its model-based clustering algorithm overcomes the drawbacks mentioned above, especially for non-Gaussian data.

In this paper, we formulate a vine copula mixture model, called *vcmm*, for continuous data allowing all types of vine tree structures, parametric pair copulas with a single parameter, and parametric margins. For simplicity, we treat the number of components as known and present well-performing solutions for the remaining model selection and parameter estimation problems. The paper is the first study in the finite mixture models literature that works with the full class of vine tree structures to the best of the authors' knowledge. It combines the flexibility of vine copulas and finite mixture models to capture complex and diverse dependence structures in the multivariate data. Another contribution of the paper is a new model-based clustering algorithm, called *vcmmc*, that incorporates realistic interdependence structures of clusters. The proposed algorithm is interpretable and allows for various shapes of the clusters. For instance, it shows how the dependence structure varies within clusters of the data.

The remainder of the paper is organized as follows. Section 2 gives an overview of vine copulas. Section 3 and Section 4 describe the vine copula mixture model and the new model-based clustering algorithm based on it. Simulation studies and analysis of real data are presented in Sections 5 and 6. Section 7 discusses our results and concludes the paper.

## 2. Vine copulas

In this section, we will recall some essential concepts of vine copulas. For more details, we refer to Chapter 3 of Joe (2014), Aas et al. (2009), and Czado (2019).

A  $d$ -dimensional copula  $C$  is a multivariate distribution on the unit hypercube  $[0, 1]^d$  with univariate uniform margins. Vine copulas are a special class of copulas based on conditioning ideas first proposed in Joe (1996) and later more developed and organized by Bedford & Cooke (2001). This approach allows any  $d$ -dimensional copula and its density to be expressed by  $\frac{d \cdot (d-1)}{2}$  bivariate copulas and their densities. Moreover, the expression can be represented by an undirected graph structure (Bedford & Cooke, 2002), i.e., *regular vine (R-vine)*. A  $d$ -dimensional R-vine consists of  $d - 1$  nested trees, each tree  $T_m$  has a node set  $V_m$ , and an edge set  $E_m$  for  $m = 1, \dots, d - 1$ . The edges in the tree level  $m$  are the nodes in the tree level  $m + 1$ , and a pair of nodes in tree  $T_{m+1}$  are allowed to be connected if they have a common node in tree  $T_m$ . A formal definition of Bedford & Cooke (2002) is that a structure  $\mathcal{V} = (T_1, \dots, T_{d-1})$  is a regular vine on  $d$  elements if it meets the following conditions:

1.  $T_1$  is a tree with node set  $V_1 = \{1, \dots, d\}$  and edge set  $E_1$ .
2.  $T_m$  is a tree with node set  $V_m = E_{m-1}$  for  $m = 2, \dots, d - 1$ .
3. (*Proximity*) If an edge connects two nodes in  $T_{m+1}$ , their associated edges in  $T_m$  must have a shared node in  $T_m$ .

The structure  $\mathcal{V} = (T_1, \dots, T_{d-1})$  is also called a *vine tree structure*, and truncating a vine after the first tree is equivalent to a Markov tree model (Brechmann et al., 2012). Thus, vines are the extending Markov trees in the sense that they allow conditional dependencies. For instance, selecting the parameters of the edges in the first tree level as correlations and the parameters of the edges in the next tree levels as partial correlations, where the partial correlations are conditioned on  $m - 1$  variables in the tree level  $m$ , in a vine can represent a multivariate Gaussian distribution when margins follow a univariate normal distribution.

Following the notation in Chapter 5 of Czado (2019), Figure 1 shows a 3-dimensional vine. The vine tree structure  $\mathcal{V}$  has two tree levels  $T_1$  and  $T_2$ . The first tree level  $T_1$  consists of the node set  $V_1 = \{1, 2, 3\}$

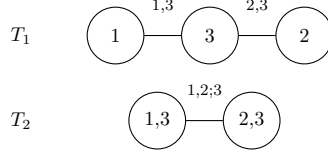


Figure 1: Example of a 3-dimensional regular vine.

and the edge set  $E_1 = \{\{1, 3\}, \{2, 3\}\}$ . In the second tree level, the node set is  $V_2 = E_1$ , and the edge set is  $E_2 = \{\{1, 2, 3\}\}$ . The two nodes in  $T_2$  are joined since they share the common node 3 in  $T_1$ .

To have a vine copula or *pair copula construction*, each edge in a vine tree structure is associated with a bivariate copula. For example, when the bivariate copulas  $C_{1,3}, C_{2,3}$  are associated with  $E_1$ , and the bivariate copula  $C_{1,3;2}$  belongs to  $E_2$  in the vine tree structure in Figure 1, a vine copula model is formed. Assume each bivariate copula  $C_{1,3}, C_{2,3}, C_{1,3;2}$  is parametric with the corresponding parameters  $\theta_{1,3}, \theta_{2,3}, \theta_{1,3;2}$  and admits the corresponding density  $c_{1,3}, c_{2,3}, c_{1,3;2}$ . Then we can write the density of this vine copula model for  $\mathbf{U} = (U_1, U_2, U_3)^\top \in [0, 1]^3$  at  $\mathbf{u} = (u_1, u_2, u_3)^\top$  as follows:

**Example 2.1.** *The density of a vine copula model corresponding to the vine tree structure in Figure 1*

$$g(u_1, u_2, u_3; \boldsymbol{\theta}) = c_{1,3}(u_1, u_3; \boldsymbol{\theta}_{1,3}) \cdot c_{2,3}(u_2, u_3; \boldsymbol{\theta}_{2,3}) \cdot c_{1,2;3}(G_{1|3}(u_1|u_3; \boldsymbol{\theta}_{1,3}), G_{2|3}(u_2|u_3; \boldsymbol{\theta}_{2,3}); u_3, \boldsymbol{\theta}_{1,2;3}), \quad (1)$$

where  $\boldsymbol{\theta} = (\boldsymbol{\theta}_{1,3}, \boldsymbol{\theta}_{2,3}, \boldsymbol{\theta}_{1,2;3})^\top$  contains all pair copula parameters, and  $G_{1|3}$  ( $G_{2|3}$ ) is the conditional distribution of the random variable  $U_1|U_3 = u_3$  ( $U_2|U_3 = u_3$ ).

Vine copulas are flexible and powerful by using bivariate building blocks (pair copulas). Moreover, Sklar's Theorem (Sklar, 1959) states another flexibility of copulas: the density of a  $d$ -dimensional distribution can be decomposed into the product of its univariate marginal densities and the associated copula density. In the remainder, assume all random variables to be absolutely continuous. Then for a  $d$ -dimensional random vector  $\mathbf{X} = (X_1, \dots, X_d)^\top \in \mathbb{R}^d$  following a joint distribution  $F$  with the univariate marginal distributions  $F_1, \dots, F_d$  and densities  $f_1, \dots, f_d$ , and a copula density  $c$  of the random vector  $\mathbf{F} = (F_1(X_1), \dots, F_d(X_D))^\top \in [0, 1]^d$ , the  $d$  dimensional joint density  $g$  can be written as

$$g(\mathbf{x}) = c(F_1(x_1), \dots, F_d(x_d)) \cdot f_1(x_1) \cdots f_d(x_d), \quad \mathbf{x} \in \mathbb{R}^d. \quad (2)$$

The vine copula model in Example 2.1 can formulate a 3-dimensional joint density  $g$  by Sklar's Theorem. Let  $F_1, F_2, F_3$  denote parametric, univariate marginal distributions with the corresponding parameters  $\gamma_1, \gamma_2, \gamma_3$ , and  $f_1, f_2, f_3$  indicate their densities.

**Example 2.2.** *The 3-dimensional joint density with the vine copula model of Example 2.1 is given by*

$$g(x_1, x_2, x_3; \boldsymbol{\psi}) = c_{1,3}(F_1(x_1; \gamma_1), F_3(x_3; \gamma_3); \boldsymbol{\theta}_{1,3}) \cdot c_{2,3}(F_2(x_2; \gamma_2), F_3(x_3; \gamma_3); \boldsymbol{\theta}_{2,3}) \cdot c_{1,2;3}(F_{1|3}(x_1|x_3; \gamma_1, \gamma_3, \boldsymbol{\theta}_{1,3}), F_{2|3}(x_2|x_3; \gamma_2, \gamma_3, \boldsymbol{\theta}_{2,3}); x_3, \boldsymbol{\theta}_{1,2;3}) \cdot f_1(x_1; \gamma_1) \cdot f_2(x_2; \gamma_2) \cdot f_3(x_3; \gamma_3), \quad (3)$$

where the vector  $\boldsymbol{\psi}$  contains the marginal and pair copula parameters,  $c_{1,2;3}(F_{1|3}(x_1|x_3), F_{2|3}(x_2|x_3); x_3)$  is the joint (copula) density corresponding to the random vector  $(F_{1|3}(X_1|X_3), F_{2|3}(X_2|X_3))^\top$  given  $X_3 = x_3$ .

In Example 2.2, it is assumed that all marginal distributions are parametric, which we assume in the following, and estimate the margins accordingly. Thus, we follow the *inference for margins* (IFM) approach (Joe & Xu, 1996). Observe that the copula density  $c_{1,2;3}$  depends on the specific value  $u_3$  of the conditioning variable  $U_3$  in Example 2.1 and the specific value  $x_3$  of the conditioning variable  $X_3$  in Example 2.2. However,

we will ignore this dependence to reduce model complexity, i.e., make the *simplifying assumption*. Under the simplifying assumption, the copula density  $c_{1,2,3}$  does not have any conditional dependence on the specific value of  $u_3$  or  $x_3$  and is a 2-dimensional copula density. Nevertheless, it still depends on the conditioning value through its arguments. For more details, we refer to Stöber et al. (2013).

**Example 2.3.** *The 3-dimensional joint density  $g$  of Example 2.2 under the simplifying assumption is given by*

$$\begin{aligned} g(x_1, x_2, x_3; \boldsymbol{\psi}) = & c_{1,3}(F_1(x_1; \boldsymbol{\gamma}_1), F_3(x_3; \boldsymbol{\gamma}_3); \boldsymbol{\theta}_{1,3}) \cdot c_{2,3}(F_2(x_2; \boldsymbol{\gamma}_2), F_3(x_3; \boldsymbol{\gamma}_3); \boldsymbol{\theta}_{2,3}) \\ & \cdot c_{1,2,3}(F_{1|3}(x_1|x_3; \boldsymbol{\gamma}_1, \boldsymbol{\gamma}_3, \boldsymbol{\theta}_{1,3}), F_{2|3}(x_2|x_3; \boldsymbol{\gamma}_2, \boldsymbol{\gamma}_3, \boldsymbol{\theta}_{2,3}); \boldsymbol{\theta}_{1,2,3}) \\ & \cdot f_1(x_1; \boldsymbol{\gamma}_1) \cdot f_2(x_2; \boldsymbol{\gamma}_2) \cdot f_3(x_3; \boldsymbol{\gamma}_3). \end{aligned} \quad (4)$$

For a general dimension  $d$ , a  $d$ -dimensional joint density is similarly constructed using  $d$  marginal densities and  $\frac{d(d-1)}{2}$  associated pair-copula densities. Let  $c_{e_a, e_b; D_e}$  be a parametric pair copula density associated with an edge  $e$  in vine tree structure  $\mathcal{V}$  and  $\boldsymbol{\theta}_{e_a, e_b; D_e}$  be its parameters ( $e \in E_m$ , for  $m = 1, \dots, d-1$ ). Let  $f_p$  denote a parametric, univariate marginal density with the parameters  $\boldsymbol{\gamma}_p$  for  $p = 1, \dots, d$ . Then a  $d$ -dimensional joint density  $g$  under the simplifying assumption can be constructed as follows:

$$\begin{aligned} g(\mathbf{x}; \boldsymbol{\psi}) = & \prod_{m=1}^{d-1} \prod_{e \in E_m} c_{e_a, e_b; D_e}(F_{e_a|D_e}(x_{e_a} | \mathbf{x}_{D_e}; \boldsymbol{\gamma}_{e_a|D_e}, \boldsymbol{\theta}_{e_a|D_e}), F_{e_b|D_e}(x_{e_b} | \mathbf{x}_{D_e}; \boldsymbol{\gamma}_{e_b|D_e}, \boldsymbol{\theta}_{e_b|D_e}); \boldsymbol{\theta}_{e_a, e_b; D_e}) \\ & \cdot \prod_{p=1}^d f_p(x_p; \boldsymbol{\gamma}_p), \end{aligned} \quad (5)$$

where  $\mathbf{x}_{D_e} = (x_z)_{z \in D_e}$  is a subvector of  $\mathbf{x} = (x_1, \dots, x_d)^\top \in \mathbb{R}^d$ , the parameter vector  $\boldsymbol{\psi}$  contains the marginal and pair copula parameters,  $F_{e_a|D_e}$  is the conditional distribution function of the random variable  $X_{e_a} | \mathbf{X}_{D_e} = \mathbf{x}_{D_e}$ . It can be calculated recursively (Joe, 1996). The marginal  $\boldsymbol{\gamma}_{e_a|D_e}$  and pair copula  $\boldsymbol{\theta}_{e_a|D_e}$  parameters are used to determine  $F_{e_a|D_e}$ . The set  $D_e$  is called the *conditioning set*, and the indices  $e_a, e_b$  form the *conditioned set*.  $D_e$  has  $m-1$  elements in the tree level  $m$ ; therefore, it is empty in the first tree.

### 3. Vine copula mixture models (vcmm)

We now introduce a vine copula mixture model (vcmm) and describe approaches for model selection and parameter estimation problems in the following subsections. The vcmm is fully parametric, i.e., works with parametric pair copulas and univariate marginal distributions.

#### 3.1. Model formulation

Suppose the data consists of  $n$  observations (samples), where an observation  $\mathbf{x}_i = (x_{i,1}, \dots, x_{i,d})^\top$  is an independent realization of a  $d$ -dimensional random vector  $\mathbf{X} = (X_1, \dots, X_d)^\top$  for  $i = 1, \dots, n$ . Assume that a mixture of  $k$  components ( $k \in \mathbb{R}^+$ ) generates the data, and the density  $g_j$  of the  $j$ th component for  $j = 1, \dots, k$  can be stated by Sklar's Theorem, as given in Equation (5). Assume that, additionally, the  $j$ th component has a mixture weight  $\pi_j$  with  $\pi_j \in (0, 1)$  for  $j = 1, \dots, k$  and  $\sum_j^k \pi_j = 1$ . Then the density of the vcmm for  $\mathbf{X} = (X_1, \dots, X_d)^\top$  at  $\mathbf{x} = (x_1, \dots, x_d)^\top$  can be written as:

$$g(\mathbf{x}; \boldsymbol{\eta}) = \sum_{j=1}^k \pi_j \cdot g_j(\mathbf{x}; \boldsymbol{\psi}_j). \quad (6)$$

Here the vector  $\boldsymbol{\psi}_j$  contains the marginal and pair copula parameters of the  $j$ th component,  $\boldsymbol{\eta}$  denotes all model parameters, i.e.,  $\boldsymbol{\eta} = (\boldsymbol{\eta}_1, \dots, \boldsymbol{\eta}_k)^\top$  and  $\boldsymbol{\eta}_j = (\pi_j, \boldsymbol{\psi}_j)^\top$  for  $j = 1, \dots, k$ .

**Example 3.1.** Vine copula mixture model formulation in 3 dimensions with 2 components

Assume data, where an observation  $\mathbf{x}_i = (x_{i,1}, x_{i,2}, x_{i,3})^\top$  for  $i = 1, \dots, n$  is given and there are two components generating the data with the mixture weights  $\pi_1 > 0$  and  $\pi_2 > 0$  ( $\pi_1 + \pi_2 = 1$ ). An observation of the first and second component is an independent realization of a 3-dimensional random vector  $\mathbf{X}_{(1)} = (X_{1(1)}, X_{2(1)}, X_{3(1)})^\top$  and  $\mathbf{X}_{(2)} = (X_{1(2)}, X_{2(2)}, X_{3(2)})^\top$ , respectively. Figure 2 shows the vine copula model of each component.  $T_{(1)1}$  and  $T_{(1)2}$  represent the first tree, whereas  $T_{(1)2}$  and  $T_{(2)2}$  refer to the second tree of the first and second component. The edge sets of the first component are  $E_{(1)1} = \{\{1, 2\}, \{2, 3\}\}$ ,  $E_{(1)2} = \{1, 3; 2\}$  and that of the second component are  $E_{(2)1} = \{\{1, 2\}, \{1, 3\}\}$ ,  $E_{(2)2} = \{2, 3; 1\}$ , respectively.

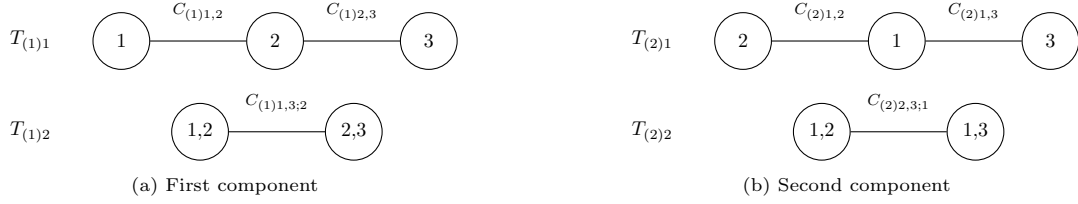


Figure 2: Vine copula model of two components.

The pair copula families and marginal distributions of both components are parametric.  $C_{(1)1,2}$ ,  $C_{(1)2,3}$ ,  $C_{(1)1,3;2}$  denote pair copula families of the first component associated with the edges in  $E_{1(1)}$  and  $E_{2(1)}$ , while  $\boldsymbol{\theta}_{(1)1,2}$ ,  $\boldsymbol{\theta}_{(1)2,3}$ ,  $\boldsymbol{\theta}_{(1)1,3;2}$  show the corresponding parameters. For the second component, we use notations  $C_{(2)1,2}$ ,  $C_{(2)1,3}$ ,  $C_{(2)2,3;1}$  for pair copula families associated with the edges in  $E_{1(2)}$  and  $E_{2(2)}$ , and  $\boldsymbol{\theta}_{(2)1,2}$ ,  $\boldsymbol{\theta}_{(2)1,3}$ ,  $\boldsymbol{\theta}_{(2)2,3;1}$  refer to the corresponding parameters. A copula density is denoted by the small  $c$  letter.  $F_{1(1/2)}$ ,  $F_{2(1/2)}$ ,  $F_{3(1/2)}$  refer to the marginal distributions of the random variables  $X_{1(1/2)}$ ,  $X_{2(1/2)}$ ,  $X_{3(1/2)}$  with the corresponding parameters  $\boldsymbol{\gamma}_{1(1/2)}$ ,  $\boldsymbol{\gamma}_{2(1/2)}$ ,  $\boldsymbol{\gamma}_{3(1/2)}$  for the first/second component. The small  $f$  letter denotes a marginal density. We can write the **density of the first component** at  $\mathbf{x} = (x_1, x_2, x_3)^\top$ :

$$\begin{aligned}
 g_1(\mathbf{x}; \boldsymbol{\psi}_1) &= c_{(1)1,2}(F_{1(1)}(x_1; \boldsymbol{\gamma}_{1(1)}), F_{2(1)}(x_2; \boldsymbol{\gamma}_{2(1)}); \boldsymbol{\theta}_{(1)1,2}) \cdot c_{(1)2,3}(F_{2(1)}(x_2; \boldsymbol{\gamma}_{2(1)}), F_{3(1)}(x_3; \boldsymbol{\gamma}_{3(1)}); \boldsymbol{\theta}_{(1)2,3}) \\
 &\quad \cdot c_{(1)1,3;2}(F_{(1)1|2}(x_1|x_2; \boldsymbol{\gamma}_{1(1)}, \boldsymbol{\gamma}_{2(1)}, \boldsymbol{\theta}_{(1)1,2}), F_{(1)3|2}(x_3|x_2; \boldsymbol{\gamma}_{3(1)}, \boldsymbol{\gamma}_{2(1)}, \boldsymbol{\theta}_{(1)2,3}); \boldsymbol{\theta}_{(1)1,3;2}) \\
 &\quad \cdot f_{1(1)}(x_1; \boldsymbol{\gamma}_{1(1)}) \cdot f_{2(1)}(x_2; \boldsymbol{\gamma}_{2(1)}) \cdot f_{3(1)}(x_3; \boldsymbol{\gamma}_{3(1)}),
 \end{aligned} \tag{7}$$

where the pair copula parameters used to determine the conditional distribution functions  $F_{(1)1|2}$  and  $F_{(1)3|2}$  are given by  $\boldsymbol{\theta}_{(1)1|2} = \boldsymbol{\theta}_{(1)1,2}$  and  $\boldsymbol{\theta}_{(1)3|2} = \boldsymbol{\theta}_{(1)2,3}$ , respectively. The marginal parameters needed for the same calculation are denoted by  $\boldsymbol{\gamma}_{(1)1|2} = (\boldsymbol{\gamma}_{1(1)}, \boldsymbol{\gamma}_{2(1)})^\top$  and  $\boldsymbol{\gamma}_{(1)3|2} = (\boldsymbol{\gamma}_{2(1)}, \boldsymbol{\gamma}_{3(1)})^\top$ . We show the marginal and pair copula parameters of the first component by  $\boldsymbol{\psi}_1 = (\boldsymbol{\gamma}_1, \boldsymbol{\theta}_1)^\top$ , where  $\boldsymbol{\gamma}_1 = (\boldsymbol{\gamma}_{1(1)}, \boldsymbol{\gamma}_{2(1)}, \boldsymbol{\gamma}_{3(1)})^\top$  and  $\boldsymbol{\theta}_1 = (\boldsymbol{\theta}_{(1)1,2}, \boldsymbol{\theta}_{(1)2,3}, \boldsymbol{\theta}_{(1)1,3;2})^\top$ . As in the first component, we can define the parameters and write the **second component density** at  $\mathbf{x} = (x_1, x_2, x_3)^\top$ :

$$\begin{aligned}
 g_2(\mathbf{x}; \boldsymbol{\psi}_2) &= c_{(2)1,2}(F_{1(2)}(x_1; \boldsymbol{\gamma}_{1(2)}), F_{2(2)}(x_2; \boldsymbol{\gamma}_{2(2)}); \boldsymbol{\theta}_{(2)1,2}) \cdot c_{(2)1,3}(F_{1(2)}(x_1; \boldsymbol{\gamma}_{1(2)}), F_{3(2)}(x_3; \boldsymbol{\gamma}_{3(2)}); \boldsymbol{\theta}_{(2)1,3}) \\
 &\quad \cdot c_{(2)2,3;1}(F_{(2)2|1}(x_2|x_1; \boldsymbol{\gamma}_{2(2)}, \boldsymbol{\gamma}_{1(2)}, \boldsymbol{\theta}_{(2)1,2}), F_{(2)3|1}(x_3|x_1; \boldsymbol{\gamma}_{3(2)}, \boldsymbol{\gamma}_{1(2)}, \boldsymbol{\theta}_{(2)1,3}); \boldsymbol{\theta}_{(2)2,3;1}) \\
 &\quad \cdot f_{1(2)}(x_1; \boldsymbol{\gamma}_{1(2)}) \cdot f_{2(2)}(x_2; \boldsymbol{\gamma}_{2(2)}) \cdot f_{3(2)}(x_3; \boldsymbol{\gamma}_{3(2)}),
 \end{aligned} \tag{8}$$

As a result, the **vine copula mixture model density** at  $\mathbf{x} = (x_1, x_2, x_3)^\top$  is given by

$$g(\mathbf{x}; \boldsymbol{\eta}) = \pi_1 g_1(\mathbf{x}; \boldsymbol{\psi}_1) + \pi_2 g_2(\mathbf{x}; \boldsymbol{\psi}_2), \tag{9}$$

where  $\boldsymbol{\eta}_1 = (\pi_1, \boldsymbol{\psi}_1)^\top$  and  $\boldsymbol{\eta}_2 = (\pi_2, \boldsymbol{\psi}_2)^\top$  indicate the model parameters of the first and second component. All model parameters are given by  $\boldsymbol{\eta} = (\boldsymbol{\eta}_1, \boldsymbol{\eta}_2)^\top$ .

### 3.2. Model selection

Vcmm inherits the problem of estimating the total number of components  $k$  hidden in the data from the finite mixture models. Moreover, due to its formulation in Equations (5) and (6), the vine tree structure  $\mathcal{V}_j$ , pair copula families  $\mathcal{B}_j(\mathcal{V}_j)$ , and marginal distributions  $\mathcal{F}_j = \{F_{1(j)}, \dots, F_{d(j)}\}$  of the  $j$ th component need to be chosen for  $j = 1, \dots, k$ . Accordingly, pair copula parameters  $\boldsymbol{\theta}_j(\mathcal{B}_j(\mathcal{V}_j))$  and marginal parameters  $\boldsymbol{\gamma}_j$  should be estimated for  $j = 1, \dots, k$ . To simplify, we will assume that the total number of components generating data is known. We will explain our approach to the remaining model selection problems in the following, and the parameter estimation is discussed in Section 3.3.

Assume a sample  $\boldsymbol{x}_i = (x_{i,1}, \dots, x_{i,d})^\top$  is assigned to a component for  $i = 1, \dots, n$ . It would be tough to determine the true samples of each component without additional information; however, we assume that we can learn model components reasonably well with our assignment. In Section 4, we will use vcmm for clustering applications and show that this method works. With the given assignment, we can first select the marginal distributions of each cluster. Because the joint density can be decomposed into univariate marginal densities and vine copula density by Sklar's Theorem, we later estimate u-data for a vine copula model by applying probability integral transformation with the estimated margins. Next, the estimated u-data is used to select the vine structure and associated pair copula families of each cluster. Assume the total number of samples assigned to the  $j$ th component is  $n_j$ , and the samples belonging to the  $j$ th component are given by  $\boldsymbol{x}_{(j)i_j} = (x_{(j)i_j,1}, \dots, x_{(j)i_j,d})^\top$  for  $i_j = 1, \dots, n_j$  and  $j = 1, \dots, k$ . It holds that  $\sum_{j=1}^k n_j = n$  and

$\bigcup_{\forall(j,i_j)} \boldsymbol{x}_{(j)i_j} = \bigcup_{\forall i} \boldsymbol{x}_i$ . Then we can summarize our steps for the model selection:

1. **Marginal distribution selection**  $\mathcal{F}_j$ : For  $p = 1, \dots, d$  and  $j = 1, \dots, k$ , the estimation of a univariate marginal distribution  $\hat{F}_{p(j)}$  can be done by using parametric or non-parametric methods. As a non-parametric approach, the empirical cumulative distribution function  $\hat{F}_{p(j)}^{emp}$  of a variable  $\boldsymbol{x}_{p(j)} = (x_{(j)1,p}, \dots, x_{(j)n_j,p})^\top$  can be fitted. For the parametric case, the log-likelihood of the marginal distribution  $F_{p(j)}$  with the density  $f_{p(j)}$  and parameters  $\boldsymbol{\gamma}_{p(j)}$  on the variable  $\boldsymbol{x}_{p(j)}$  is given by

$$\ell(\boldsymbol{\gamma}_{p(j)}) = \sum_{i=1}^{n_j} \log(f_{p(j)}(x_{(j)i,p}; \boldsymbol{\gamma}_{p(j)})) \quad \text{for } p = 1, \dots, d \quad \text{and } j = 1, \dots, k. \quad (10)$$

The Akaike information criterion (AIC) (Akaike, 1998), a commonly used model selection criteria, is given by

$$AIC(\boldsymbol{\gamma}_{p(j)}) = -2 \cdot \ell(\boldsymbol{\gamma}_{p(j)}) + 2 \cdot |\boldsymbol{\gamma}_{p(j)}| \quad \text{for } p = 1, \dots, d \quad \text{and } j = 1, \dots, k, \quad (11)$$

where  $|\boldsymbol{\gamma}_{p(j)}|$  refers to the number of marginal parameters in  $F_{p(j)}$ . For each candidate for marginal distribution on the variable  $\boldsymbol{x}_{p(j)}$ , we first find the parameters that maximize the log-likelihood  $\ell(\hat{\boldsymbol{\gamma}}_{p(j)})$ , then the marginal distribution with the lowest AIC is selected. The estimated margins  $\hat{F}_{p(j)}$  are then used to obtain the u-data of the  $j$ th component by applying probability integral transformation:  $\hat{\boldsymbol{u}}_{p(j)} = \hat{F}_{p(j)}(\boldsymbol{x}_{p(j)}; \hat{\boldsymbol{\gamma}}_{p(j)})$  for a parametric margin and  $\hat{\boldsymbol{u}}_{p(j)} = \hat{F}_{p(j)}^{emp}(\boldsymbol{x}_{p(j)})$  for a non-parametric margin. It holds  $\hat{\boldsymbol{u}}_{p(j)} = (\hat{u}_{(j)1,p}, \dots, \hat{u}_{(j)n_j,p})^\top$ .

2. **Vine tree structure selection**  $\mathcal{V}_j$ : For  $j = 1, \dots, k$ , the best selection of  $\mathcal{V}_j$  would be the true structure selection, but the total number of vine tree structures on  $d$  variables is  $\frac{d!}{2} \cdot 2^{\binom{d-2}{2}}$  (Morales-Nápoles, 2010). If  $d$  is small, it is possible to enumerate all possible structures. However, it is not a feasible approach for us even with small dimensions as we need to select pair copula families and estimate model parameters for each scenario. Therefore, we use the greedy algorithm of Dißmann et al. (2013). This approach proceeds sequentially tree by tree, starting from the tree level 1 and finds the maximum spanning tree at each tree level. Edge weight is the absolute Kendall's  $\tau$  value between the pair of nodes forming the edge. The algorithm preserves the R-vine definition introduced in Section 2.

3. **Pair copula family selection**  $\mathcal{B}_j(\mathcal{V}_j)$ : For  $j = 1, \dots, k$ , after learning the vine tree structure, pair copula families of the given structure can be estimated sequentially tree by tree, as proposed in Dißmann et al. (2013). For a parametric pair copula  $C_{(j)e_a, e_b; D_e}$  associated with an edge  $e$  in  $\mathcal{V}_j$  with the density  $c_{(j)e_a, e_b; D_e}$  and parameters  $\boldsymbol{\theta}_{(j)e_a, e_b; D_e}$ , we first estimate the parameters that maximize the log-likelihood  $\ell(\hat{\boldsymbol{\theta}}_{(j)e_a, e_b; D_e})$ . Later we choose the copula family with the lowest AIC:

$$AIC(\boldsymbol{\theta}_{(j)e_a, e_b; D_e}) = -2 \cdot \ell(\boldsymbol{\theta}_{(j)e_a, e_b; D_e}) + 2 \cdot |\boldsymbol{\theta}_{(j)e_a, e_b; D_e}| \quad \text{for } j = 1, \dots, k \quad \text{and } e \in \mathcal{V}_j, \quad (12)$$

where  $|\boldsymbol{\theta}_{(j)e_a, e_b; D_e}|$  denotes the number of copula parameters in  $c_{(j)e_a, e_b; D_e}$ .

### 3.3. Parameter estimation

Given that the marginal distributions, vine tree structure, and associated pair copula families of each component are selected and known, a first task in the vcmm is to estimate the model parameters  $\boldsymbol{\eta}$  in Equation (6). The optimal parameter estimates would be the values that maximize the log-likelihood of the given data defined in Equation (13):

$$\ell(\boldsymbol{\eta}) = \log \prod_{i=1}^n g(\mathbf{x}_i; \boldsymbol{\psi}) = \log \prod_{i=1}^n \sum_{j=1}^k \pi_j \cdot g_j(\mathbf{x}_i; \boldsymbol{\psi}_j). \quad (13)$$

Nevertheless, the true assignment of the observations to each component is unknown, and the parameter estimates would change depending on the component to which an observation belongs. As a solution to this problem, the expectation-maximization (EM) algorithm (Dempster et al., 1977) views the observations  $\mathbf{x}_i = (x_{i,1}, \dots, x_{i,d})^\top$  as incomplete and introduces latent variables  $\mathbf{z}_i = (z_{i,1}, \dots, z_{i,k})^\top$ , where each element  $z_{i,j}$  is a binary variable defined as

$$z_{i,j} = \begin{cases} 1, & \text{if } \mathbf{x}_i \text{ belongs to the } j\text{th component,} \\ 0, & \text{otherwise,} \end{cases} \quad (14)$$

and  $\sum_{j=1}^k z_{i,j} = 1$ . The random vector  $\mathbf{Z}_i$  corresponding to  $\mathbf{z}_i$  follows a multinomial distribution with  $k$  trials and probabilities  $\pi_1, \dots, \pi_k$ , that is,  $\mathbf{Z}_i \sim \text{Mult}(k, \boldsymbol{\pi} = (\pi_1, \dots, \pi_k))$ . Then we can write the *complete data log-likelihood*  $\ell_c(\boldsymbol{\eta}; \mathbf{z}, \mathbf{x})$  of the complete data  $\mathbf{y}_i = (\mathbf{x}_i, \mathbf{z}_i)^\top$  from Equation (6) as:

$$\ell_c(\boldsymbol{\eta}; \mathbf{z}, \mathbf{x}) = \log \prod_{i=1}^n \prod_{j=1}^k [\pi_j \cdot g_j(\mathbf{x}_i; \boldsymbol{\psi}_j)]^{z_{i,j}} = \sum_{i=1}^n \sum_{j=1}^k z_{i,j} \cdot \log \pi_j + \sum_{i=1}^n \sum_{j=1}^k z_{i,j} \cdot \log g_j(\mathbf{x}_i; \boldsymbol{\psi}_j), \quad (15)$$

where  $g_j(\mathbf{x}_i; \boldsymbol{\psi}_j)$  is given in Equation (5). Hence, we can write:

$$\begin{aligned} \ell_c(\boldsymbol{\eta}; \mathbf{z}, \mathbf{x}) &= \sum_{i=1}^n \sum_{j=1}^k [z_{i,j} \cdot \log \pi_j] + \sum_{i=1}^n \sum_{j=1}^k \sum_{p=1}^d [z_{i,j} \cdot \log f_{p(j)}(x_{i,p}; \boldsymbol{\gamma}_{p(j)})] \\ &+ \sum_{i=1}^n \sum_{j=1}^k \sum_{m=1}^{d-1} \sum_{e \in E_{(j)m}} [z_{i,j} \cdot \log c_{(j)e_a, e_b; D_e}(F_{(j)e_a | D_e}(x_{i,e_a} | \mathbf{x}_{i, D_e}; \boldsymbol{\gamma}_{(j)e_a | D_e}, \boldsymbol{\theta}_{(j)e_a | D_e}), \\ &F_{(j)e_b | D_e}(x_{i,e_b} | \mathbf{x}_{i, D_e}; \boldsymbol{\gamma}_{(j)e_b | D_e}, \boldsymbol{\theta}_{(j)e_b | D_e}); \boldsymbol{\theta}_{(j)e_a, e_b; D_e})]. \end{aligned} \quad (16)$$

Note that we use  $\boldsymbol{\theta}_j$  for the pair copula parameters instead of  $\boldsymbol{\theta}_j(\mathcal{B}_j(\mathcal{V}_j))$  for easier notation.

The EM algorithm repeatedly alternates the E and M steps, increasing the data log-likelihood at each iteration (Dempster et al., 1977). The E-step requires calculating the conditional expectation of the complete-data log likelihood, given the observed data and current parameter estimates. The M-step maximizes the expected complete data log-likelihood from the E-step over all parameters. We need to estimate marginal

parameters  $\gamma_j$ , pair copula parameters  $\theta_j$ , and mixture weight  $\pi_j$  of the  $j$ th component. Since their joint estimation is not tractable and efficient, we use the expectation conditional maximum (ECM) algorithm (Meng & Rubin, 1993). With the ECM, we replace the M-step in the EM with three lower dimensional maximization problems called CM-steps. Our steps at the  $(t + 1)$ th iteration are given by

1. **E-step** (*Posterior probabilities*): Calculate the posterior probability that an observation  $\mathbf{x}_i$  belongs to the  $j$ th component given the current values of the model parameters  $\pi_j^{(t)}$  and  $\boldsymbol{\psi}_j^{(t)} = (\boldsymbol{\gamma}_j^{(t)}, \boldsymbol{\theta}_j^{(t)})^\top$ :

$$r_{i,j}^{(t+1)} = \frac{\pi_j^{(t)} g_j(\mathbf{x}_i; \boldsymbol{\psi}_j^{(t)})}{\sum_{j=1}^k \pi_j^{(t)} g_j(\mathbf{x}_i; \boldsymbol{\psi}_j^{(t)})} \quad \text{for } i = 1, \dots, n \quad \text{and } j = 1, \dots, k. \quad (17)$$

2. **CM-step 1** (*Mixture weights*): Maximize  $\ell_c(\boldsymbol{\eta}; \mathbf{z}, \mathbf{x})$  over  $\pi_j$  given the updated posterior probabilities  $r_{i,j}^{(t+1)}$ :

$$\pi_j^{(t+1)} = \arg \max_{\pi_j} \sum_{i=1}^n r_{i,j}^{(t+1)} \cdot \log \pi_j \quad \text{for } j = 1, \dots, k. \quad (18)$$

A closed form solution exists and is given by

$$\pi_j^{(t+1)} = \frac{\sum_{i=1}^n r_{i,j}^{(t+1)}}{n} \quad \text{for } j = 1, \dots, k. \quad (19)$$

3. **CM-step 2** (*Marginal parameters*): Optimal marginal parameter estimates  $\gamma_j^*$  of the  $j$ th component would maximize  $\ell_c(\boldsymbol{\eta}; \mathbf{z}, \mathbf{x})$  over  $\gamma_j$  given the current values of the pair copula parameters  $\boldsymbol{\theta}_j^{(t)}$  and updated posterior probabilities  $r_{i,j}^{(t+1)}$ :

$$\gamma_j^* = \arg \max_{\gamma_j} \sum_{i=1}^n r_{i,j}^{(t+1)} \cdot \log g_j(\mathbf{x}_i; \gamma_j, \boldsymbol{\theta}_j^{(t)}) \quad \text{for } j = 1, \dots, k. \quad (20)$$

However, since a closed form solution does not exist, we numerically maximize  $\ell_c(\boldsymbol{\eta}; \mathbf{z}, \mathbf{x})$  over  $\gamma_j$

$$\max_{\gamma_j} \sum_{i=1}^n r_{i,j}^{(t+1)} \cdot \log g_j(\mathbf{x}_i; \gamma_j, \boldsymbol{\theta}_j^{(t)}) \quad \text{for } j = 1, \dots, k \quad (21)$$

to find the updated values of the marginal parameters  $\gamma_j^{(t+1)}$ .

4. **CM-step 3** (*Pair copula parameters*): As in the marginal parameters estimation, a closed form solution that maximizes  $\ell_c(\boldsymbol{\eta}; \mathbf{z}, \mathbf{x})$  over  $\boldsymbol{\theta}_j$  given the current values of the marginal parameters  $\gamma_j^{(t+1)}$  and updated posterior probabilities  $r_{i,j}^{(t+1)}$  does not exist. Hence, one could numerically maximize  $\ell_c(\boldsymbol{\eta}; \mathbf{z}, \mathbf{x})$  over  $\boldsymbol{\theta}_j$

$$\max_{\boldsymbol{\theta}_j} \sum_{i=1}^n r_{i,j}^{(t+1)} \cdot \log g_j(\mathbf{x}_i; \gamma_j^{(t+1)}, \boldsymbol{\theta}_j) \quad \text{for } j = 1, \dots, k \quad (22)$$

to find the updated values of the pair copula parameters  $\boldsymbol{\theta}_j^{(t+1)}$ . Nevertheless, the joint log-likelihood optimization of a  $d$ -dimensional, parametric vine copula with pair copulas with a single parameter requires a maximization over  $\frac{d \cdot (d-1)}{2}$  parameters. Because it grows quadratically in dimension  $d$ , we suggest using a sequential parameter estimation approach given a vine tree structure and pair copula families, as in the greedy algorithm of Dißmann et al. (2013). We have the following modification to CM-step 3, which we call CMR-step.

5. **CMR-step** (*Pair copula parameters updated sequentially*): Alternatively, we can estimate the pair copula parameters sequentially tree by tree, starting from the tree level 1 given the vine tree structure and pair copula families. For more details, we refer to Chapter 7 of [Czado \(2019\)](#). We can rewrite the optimization problem given in Equation (22) by using Equation (16) as

$$\begin{aligned} \max_{\boldsymbol{\theta}_j} \sum_{i=1}^n \sum_{m=1}^{d-1} \sum_{e \in E_{(j)m}} r_{i,j}^{(t+1)} \cdot \log c_{(j)e_a, e_b; D_e} (F_{(j)e_a | D_e} (x_{i,e_a} | \mathbf{x}_{i,D_e}; \boldsymbol{\gamma}_{(j)e_a | D_e}^{(t+1)}, \boldsymbol{\theta}_{(j)e_a | D_e}), \\ F_{(j)e_b | D_e} (x_{i,e_b} | \mathbf{x}_{i,D_e}; \boldsymbol{\gamma}_{(j)e_b | D_e}^{(t+1)}, \boldsymbol{\theta}_{(j)e_b | D_e}); \boldsymbol{\theta}_{(j)e_a, e_b; D_e}) \quad \text{for } j = 1, \dots, k. \end{aligned} \quad (23)$$

We first update the values of the pair copula parameters  $\boldsymbol{\theta}_j^{(t+1)}(T_1)$  in the tree level 1 ( $m = 1$ ). Since  $D_e$  is empty in the first tree, as discussed in Section 2, we start by solving the following problem

$$\max_{\boldsymbol{\theta}_j(T_1)} \sum_{i=1}^n \sum_{e \in E_{(j)1}} r_{i,j}^{(t+1)} \cdot \log c_{(j)e_a, e_b} (F_{(j)e_a} (x_{i,e_a}; \boldsymbol{\gamma}_{(j)e_a}^{(t+1)}), F_{(j)e_b} (x_{i,e_b}; \boldsymbol{\gamma}_{(j)e_b}^{(t+1)}); \boldsymbol{\theta}_{(j)e_a, e_b}) \quad \text{for } j = 1, \dots, k \quad (24)$$

to obtain  $\boldsymbol{\theta}_j^{(t+1)}(T_1)$ . Then these values are used to calculate the conditional distributions  $F_{(j)e_a | D_e}$ ,  $F_{(j)e_b | D_e}$  and their observations we need in the tree level 2. More details and examples of these calculations can be found in [Aas et al. \(2009\)](#) and Chapter 4 of [Czado \(2019\)](#). Later we update the values of the pair copula parameters in the second tree with the weights  $r_{i,j}^{(t+1)}$  and obtain  $\boldsymbol{\theta}_j^{(t+1)}(T_2)$ . We proceed with this way up to the last tree level  $m - 1$ . The CMR-step does not guarantee that the data log-likelihood increases at each iteration, but our experiments showed that this is rare.

### Starting values and stopping condition

Since the ECM is an iterative algorithm, we require initial parameters  $\boldsymbol{\eta}_j^{(0)}$  of the  $j$ th component for  $j = 1, \dots, k$ . However, it is sensitive to the starting values, and a poor choice of them may result in convergence to a local maximum as an EM-type algorithm ([Karlis & Xekalaki, 2003](#)). To have different initial partitions, we perform a mixture of multivariate Gaussian distributions (GMM) and k-means clustering of the given observations  $\mathbf{x}_i = (x_{i,1}, \dots, x_{i,d})^\top$  for  $i = 1, \dots, n$ . Assume that the total number of observations assigned to the  $j$ th component at the 0th iteration is  $n_j^{(0)}$ , and the observations belonging to the  $j$ th component at the 0th iteration are given by  $\mathbf{x}_{(j)i_j}^{(0)} = (x_{(j)i_j,1}^{(0)}, \dots, x_{(j)i_j,d}^{(0)})^\top$  for  $i_j = 1, \dots, n_j^{(0)}$  and  $j = 1, \dots, k$ . It holds that  $\sum_{j=1}^k n_j^{(0)} = n$  and  $\bigcup_{\forall (j,i_j)} \mathbf{x}_{(j)i_j}^{(0)} = \bigcup_{\forall i} \mathbf{x}_i$ . Then our starting values for the parameters are:

1. Initial marginal parameters  $\boldsymbol{\gamma}_{p(j)}^{(0)}$ : For  $j = 1, \dots, k$  and  $p = 1, \dots, d$ , they maximize the log-likelihood of a variable  $\mathbf{x}_{p(j)}^{(0)} = (x_{(j)1,p}^{(0)}, \dots, x_{(j)n_j^{(0)},p}^{(0)})^\top$  given in Equation (10) and as described in Section 3.2.
2. Initial pair copula parameters  $\boldsymbol{\theta}_{(j)}^{(0)}$ : For  $j = 1, \dots, k$  and  $p = 1, \dots, d$ , first, the empirical cumulative distribution function  $F_{p(j)}^{emp(0)}$  of a variable  $\mathbf{x}_{p(j)}^{(0)}$  is fitted to obtain u-data of the  $j$ th component by applying the probability integral transformation,  $\mathbf{u}_{p(j)}^{(0)} = F_{p(j)}^{emp(0)}(\mathbf{x}_{p(j)}^{(0)})$ . Then the estimated u-data is used to select a vine tree structure and the associated pair copula families with their parameters, as discussed in the CRM-step in Section 3.2.
3. Initial mixture weights  $\pi_{(j)}^{(0)}$ : For  $j = 1, \dots, k$ , they are proportional to the total number observations belonging to the  $j$ th component and given by  $\pi_{(j)}^{(0)} = \frac{n_j^{(0)}}{n}$ .

Our stopping criterion terminates the algorithm when either the relative difference in the data log-likelihood between two successive iterations is less than the desired tolerance or the data log-likelihood at one iteration

is smaller than the data log-likelihood at the previous iteration. The latter can result from the CRM-step, as discussed before. We use the following criteria in our simulation studies and real data analysis for clustering:

$$\begin{aligned}
1. \quad & \frac{\ell(\boldsymbol{\eta}^{(t+1)}) - \ell(\boldsymbol{\eta}^{(t)})}{\ell(\boldsymbol{\eta}^{(t)})} < 0.001 \quad \text{for } t = 1, \dots, (s-1) \quad \text{or} \\
2. \quad & \ell(\boldsymbol{\eta}^{(t+1)}) < \ell(\boldsymbol{\eta}^{(t)}) \quad \text{for } t = 1, \dots, (s-1).
\end{aligned} \tag{25}$$

#### 4. Model-based clustering algorithm: `vcmmc`

In this section, we will formulate a model-based clustering algorithm (`vcmmc`) with vine copula mixture models that we introduced in Section 3. We provide our pseudo code in Algorithm 1. It consists of 7 primary building blocks and implements them in R (R Core Team, 2019). The first step, initial clustering assignment, partitions observations  $\mathbf{x}_i = (x_{i,1}, \dots, x_{i,d})^\top$  for  $i = 1, \dots, n$  into  $k$  components (clusters) using a predetermined clustering algorithm. In our approach, we perform GMM using the package `mclust` (Scrucca et al., 2016) and k-means clustering using the package `stats`. We use their default specifications, but fix the total number of clusters.

As a second step, we select the `vcmmc` components, as discussed in Section 3.2. For the estimation of marginal distributions and associated parameters, we work with the package `fitdistrplus` and its function `fitdist` (Delignette-Muller & Dutang, 2015). Currently, we assume that a univariate margin follows either normal or gamma distribution. Thus, the total number of marginal parameter estimates per cluster is  $2 \cdot d$ . Note that exponential distribution is a particular case of the gamma distribution, and further marginal distributions can easily be incorporated into our algorithm. However, its current version can estimate the marginal distributions of the real data sets reasonably well, as shown in Section 6. For the selection of vine copula models, we first truncate a vine tree structure at the tree level 1, thereby obtaining a Markov tree model. Assuming all pair copula families are parametric with a single parameter, the total number of vine copula parameter estimates per cluster is  $d-1$  with a Markov tree; however, it is  $\frac{d \cdot (d-1)}{2}$  with a full vine specification. Thus, working with Markov trees allows us to decrease the size of the optimization problem (CMR-step in Section 3.3) from quadratic to linear in dimension  $d$ . The pair copula families used in our algorithm are parametric with a single parameter: Gaussian, Clayton, Gumbel, Frank, and Joe copula. Since we apply their possible rotations, the total number of pair copula families utilized is 14. Chapter 3 of Czado (2019) provides more details about them. For this part, we work with the package `VineCopula` and mainly its function `RVineStructureSelect` (Nagler et al., 2019).

The third step, iterative parameter estimation, updates the `vcmmc` parameters numerically until a stopping condition holds, as explained in Section 3.3. Assume it stops after  $s$  iterations. Then the total number of updated parameters up to this point is  $3 \cdot k \cdot s \cdot d$  (obtained by  $k \cdot s \cdot (2 \cdot d + d - 1 + 1)$ ), which is linear in dimension  $d$ , the total number of clusters  $k$ , and iterations  $s$ .

Next, we partition the samples into  $k$  clusters with the updated posterior probabilities as a temporary clustering assignment. A sample is a member of the cluster, where its posterior probability is highest.

Because dependencies can exist in higher tree levels, and accounting those can improve the model power, the final `vcmmc` model is based on a full vine specification. The fifth step, temporary model selection with full vine specification, estimates the model components, including all possible vine tree levels and its parameters with the clustering assignment of Step IV. The total number of updated parameters with this step is  $k \cdot (3 \cdot s \cdot d + 2 \cdot d + \frac{d \cdot (d-1)}{2} + 1)$ , which is linear in the total number of clusters  $k$  and iterations  $s$  and quadratic in dimension  $d$ . The total number of free parameters at this step is  $k \cdot (2 \cdot d + \frac{d \cdot (d-1)}{2}) + k - 1$ , where  $k - 1$  accounts for the mixture weights of the clusters. Note that using full vine specification introduces additional parameter estimates and cannot always give the best clustering partition, as discussed in Section 6.2. Thus, we will study the problem of *finding the optimal truncation level in the `vcmmc`* in future research.

Next, we run the steps we have explained until now with the clustering assignment of the k-means and GMM separately. We will show the benefits and need for this step with our simulation studies in Section 5. The sixth step, final model selection with different initial clustering methods, chooses the best model in the

vmmc using Bayesian Information Criteria (BIC) (Schwarz, 1978):

$$BIC(\boldsymbol{\eta}) = -2 \cdot \ell(\boldsymbol{\eta}) + |\boldsymbol{\eta}| \cdot \log(n), \quad (26)$$

where  $\ell(\boldsymbol{\eta})$  is the data log-likelihood,  $|\boldsymbol{\eta}|$  refers to the total number of free parameters in the model, and  $n$  denotes the total number of observations. The model with a smaller BIC value is preferred because we do not know the actual cluster labels of the observations used as a comparison criterion. The BIC value tends to select a model that reasonably approximates the density; however, the model does not always give a good clustering partition. Such model examples can be found in Scrucca et al. (2016) and Punzo & McNicholas (2016). Besides, we will draw a similar conclusion in our simulation studies in Section 5. Another criterion that we could use for the model selection would be integrated completed likelihood (ICL) (Biernacki et al., 2000). Since we did not observe significant differences in the model preference of the BIC value and ICL in our experiments, we work with the BIC value and report the results in Sections 5 and 6 accordingly.

The last step, the final clustering assignment, assigns the observations to the clusters with the winner model's final posterior probabilities. The winner model gives the final model components and parameter estimates of the vmmc.

---

**Algorithm 1** Vine copula mixture models clustering: vmmc

---

- 1: **Input:**  $d$ -dimensional  $n$  observations to cluster  $\mathbf{x}_i = (x_{i,1}, \dots, x_{i,d})^\top \in \mathbb{R}^d$  for  $i = 1, \dots, n$  and total number of clusters  $k$ .
  - 2: **Output:** A clustering partition of the observations  $\mathcal{C} = \{\mathcal{C}_1, \dots, \mathcal{C}_k\}$ , estimated model components and parameters of the  $j$ th cluster defined in Section 3  $\hat{\mathcal{F}}_j, \hat{\boldsymbol{\gamma}}_j, \hat{\mathcal{V}}_j, \hat{\mathcal{B}}_j(\hat{\mathcal{V}}_j), \hat{\boldsymbol{\theta}}_j(\hat{\mathcal{B}}_j(\hat{\mathcal{V}}_j)), \hat{\pi}_j$  for  $j = 1, \dots, k$ .
  - 3: **for**  $j = 1, \dots, k$  **do**
  - 4:   **Step I: Initial clustering assignment**
  - 5:    $\mathbf{x}_{(j)i_j}^{(0)} = (x_{(j)i_j,1}^{(0)}, \dots, x_{(j)i_j,d}^{(0)})^\top$  for  $i_j = 1, \dots, n_j^{(0)}$ ,  $\sum_{j=1}^k n_j^{(0)} = n$  and  $\bigcup_{\forall(j,i_j)} \mathbf{x}_{(j)i_j}^{(0)} = \bigcup_{\forall i} \mathbf{x}_i$ .
  - 6:   **Step II: Initial model selection with Markov tree**
  - 7:   **for**  $p = 1, \dots, d$  **do**
  - 8:      $\mathbf{x}_{p(j)}^{(0)} = (x_{(j)1,p}^{(0)}, \dots, x_{(j)n_j^{(0)},p}^{(0)})^\top$ ,
  - 9:      $F_{p(j)}^{emp(0)} \leftarrow$  empirical distribution function of  $\mathbf{x}_{p(j)}^{(0)}$ ,
  - 10:      $\mathbf{u}_{p(j)}^{(0)} = F_{p(j)}^{emp(0)}(\mathbf{x}_{p(j)}^{(0)})$ ,
  - 11:      $(F_{p(j)}^{(0)}, \boldsymbol{\gamma}_{p(j)}^{(0)}) \leftarrow \arg \min_{fam, \boldsymbol{\gamma}} fitdist(\mathbf{x}_{p(j)}^{(0)}, fam) \$ AIC$ , where  $fam \in \{\text{normal, gamma}\}$ ,
  - 12:      $\mathbf{u}_{(j)}^{(0)} = (\mathbf{u}_{1(j)}^{(0)}, \dots, \mathbf{u}_{d(j)}^{(0)})^\top$ ,
  - 13:      $bicop \in \{\text{Gaussian, Clayton, Gumbel, Frank, Joe}\}$ ,
  - 14:      $\pi_j^{(0)} \leftarrow \frac{n_j^{(0)}}{n}$ ,
  - 15:      $model_{markov} \leftarrow RVineStructureSelect(\mathbf{u}_{(j)}^{(0)}, bicop, trunclevel = 1)$ ,
  - 16:      $\mathcal{V}_j^{(0)} \leftarrow model_{markov} \$ Matrix$  and  $\mathcal{B}_j^{(0)} \leftarrow model_{markov} \$ Family$  and  $\boldsymbol{\theta}_j^{(0)} \leftarrow model_{markov} \$ par$ .
  - 17: **Step III: Iterative parameter estimation**
  - 18: **while** stop=FALSE **do**
  - 19:    $t \leftarrow 0$ ,
  - 20:   **for**  $j = 1, \dots, k$  **do**
  - 21:     Update  $r_{i,j}^{(t+1)}$  as in Equation (17) for  $i = 1, \dots, n$ ,
  - 22:     Update  $\pi_j^{(t+1)}, \boldsymbol{\gamma}_j^{(t+1)}$  and  $\boldsymbol{\theta}_j^{(t+1)}$  sequentially as in Equation (19), (21) and (23), respectively,
  - 23:    $t \leftarrow t + 1$ ,
  - 24:   **if** a termination criterion in Equation (25) holds **then**
  - 25:      $s \leftarrow t$ , stop=TRUE and **break**.
-

---

26: **Step IV: Temporary clustering assignment**

27:  $\mathbf{x}_i \in \mathcal{C}_{j^*} \iff j^* = \arg \max_{j=1, \dots, k} r_{i,j}^{(s)}$  for  $i = 1, \dots, n$ .

28: **for**  $j = 1, \dots, k$  **do**

29:  $\mathbf{x}_{(j)i_j}^{(s+1)} = (x_{(j)i_j,1}^{(s+1)}, \dots, x_{(j)i_j,d}^{(s+1)})^\top$  for  $i_j = 1, \dots, n_j^{(s+1)}$ ,  $\sum_{j=1}^k n_j^{(s+1)} = n$  and  $\bigcup_{\forall (j,i_j)} \mathbf{x}_{(j)i_j}^{(s+1)} = \bigcup_{\forall i} \mathbf{x}_i$ .

30: **Step V: Temporary model selection with full vine specification**

31: Perform lines 7–13 with the new assignment  $\mathbf{x}_{(j)i_j}^{(s+1)}$  and change the iteration index from (0) to (s+1),

32:  $\pi_j^{(s+1)} \leftarrow \frac{\sum_{i=1}^n r_{i,j}^{(s+1)}}{n}$ , where  $r_{i,j}^{(s+1)}$  is calculated by Equation (17),

33:  $model_{vcmm} \leftarrow RVineStructureSelect(\mathbf{u}_{(j)}^{(s+1)}, bicop, trunclevel = d - 1)$ ,

34:  $\mathcal{V}_j^{(s+1)} \leftarrow model_{vcmm}\$Matrix$  and  $\mathcal{B}_j^{(s+1)} \leftarrow model_{vcmm}\$Family$  and  $\theta_j^{(s+1)} \leftarrow model_{vcmm}\$par$ .

35: **Step VI: Final model selection with different initial clustering methods**

36: Perform the lines 3–34 with a different initial clustering method and find its assignment at line 4 and 5,

37: Choose the winner model with the lowest BIC value.

38: **Step VII: Final clustering assignment**

39:  $\mathbf{x}_i \in \mathcal{C}_{j^*} \iff j^* = \arg \max_{j=1, \dots, k} r_{i,j}^{(s+2)}$  for  $i = 1, \dots, n$ , where  $r_{i,j}^{(s+2)}$  are the posterior probabilities of the winner model with the lowest BIC value.

40:  $\hat{\mathcal{F}}_j \leftarrow \{F_{1(j)}^{(s+1)}, \dots, F_{d(j)}^{(s+1)}\}$ ,  $\hat{\gamma}_j \leftarrow \{\gamma_{1(j)}^{(s+1)}, \dots, \gamma_{d(j)}^{(s+1)}\}$ ,  $\hat{\mathcal{V}}_j \leftarrow \mathcal{V}_j^{(s+1)}$ ,  $\hat{\mathcal{B}}_j(\hat{\mathcal{V}}_j) \leftarrow \mathcal{B}_j^{(s+1)}$ ,  $\hat{\theta}_j(\hat{\mathcal{B}}_j(\hat{\mathcal{V}}_j)) \leftarrow \theta_j^{(s+1)}$ ,  $\hat{\pi}_j \leftarrow \pi_j^{(s+1)}$ , where the components and parameters at the (s+1)th iteration belong to the winner model with the lowest BIC value.

---

## 5. Simulation studies

In this section, we will demonstrate promising results of our clustering algorithm, `vcmmc`, using simulated data and compare its performance with some well-known model-based clustering algorithms: GMM, the mixture of multivariate skew normal, t, and skew-t distributions. We fit the GMM using the package `mclust` and the others using the package `mixsmsn` (Prates et al., 2013). We work with default specifications of the packages, but specify the total number of clusters. For the clustering performance evaluation, we use the BIC value and misclassification rate when the true labels are available. The lower the BIC value or misclassification rate, the better the clustering assignment.

The simulated data has 3 variables, 2 clusters, and either 100 or 500 observations in each cluster, and we replicate their data generating process 100 times.  $X_{p(1)} = F_{p(1)}^{-1}(U_{p(1)}; \gamma_{p(1)})$  and  $X_{p(2)} = F_{p(2)}^{-1}(U_{p(2)}; \gamma_{p(2)})$  for  $p = 1, 2, 3$  give the variables of the first and second clusters, respectively. We simulate  $U_{p(1)}$  and  $U_{p(2)}$  from a specified vine copula model and chosen  $F_{p(1)}, F_{p(2)}, \gamma_{p(1)}, \gamma_{p(2)}$ . A mixture of vine copulas generates the first scenario in Section 5.1 with Gaussian dependencies and non-Gaussian margins, whereas the second case in Section 5.2 simulates data from a mixture of vine copulas with non-Gaussian dependencies and Gaussian/non-Gaussian margins. We aim to analyze how well the evaluated algorithms capture different dependence structures and shapes hidden in the multivariate data with diverse sample sizes.

### 5.1. The mixture of vine copulas with Gaussian dependencies and non-Gaussian margins

We simulate data  $U_{p(1)}$  and  $U_{p(2)}$  for  $p = 1, 2, 3$  from a vine copula model, where all pair copula families are Gaussian, as shown in Figure 3. Both clusters include positive and negative, as well as medium and high strength dependencies.

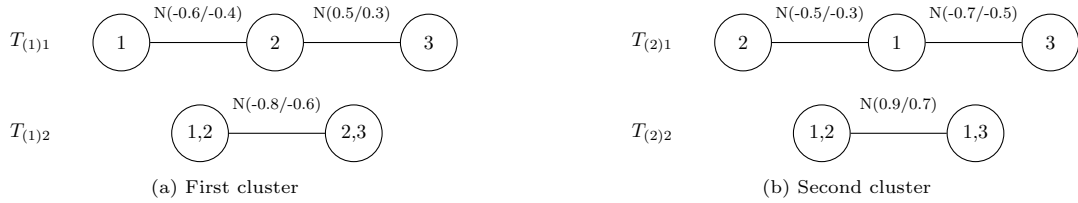


Figure 3: Vine tree structure of simulated data with Gaussian pair copulas and two clusters. A capital letter  $N$  at an edge refers to the Gaussian copula. The true parameter value and corresponding Kendall's  $\tau$  of the pair copula are given inside the parenthesis (parameter/Kendall's  $\tau$ ).

Then we transform the data from u-scale  $U_{p(1)}, U_{p(2)}$  to x-scale  $X_{p(1)}, X_{p(2)}$  as explained before. Table 1 presents the marginal distributions with the parameters, and Figure 4 visualizes the effect of the non-Gaussian margins on the shape of multivariate data. We present the scatter plots of exemplary data (1000 observations) on the x-scale, and observations of the same cluster have the same color. Its samples on  $X_1$  and  $X_3$  plane cannot partition the data; however, a plane with  $X_2$  can separate them.

|                           |                           |                           |                           |                           |                           |
|---------------------------|---------------------------|---------------------------|---------------------------|---------------------------|---------------------------|
| $F_{1(1)}(\gamma_{1(1)})$ | $F_{2(1)}(\gamma_{2(1)})$ | $F_{3(1)}(\gamma_{3(1)})$ | $F_{1(2)}(\gamma_{1(2)})$ | $F_{2(2)}(\gamma_{2(2)})$ | $F_{3(2)}(\gamma_{3(2)})$ |
| $\Gamma(5, 3.5)$          | $Exp(0.9)$                | $Exp(2.5)$                | $\Gamma(2, 0.8)$          | $\Gamma(6, 4)$            | $Exp(0.5)$                |

Table 1: Univariate marginal distributions and associated parameters of each cluster.  $\Gamma(\alpha, \beta)$  refers to the gamma distribution with shape parameter  $\alpha$  and rate parameter  $\beta$ ,  $Exp(\lambda)$  denotes the exponential distribution with rate parameter  $\lambda$ .

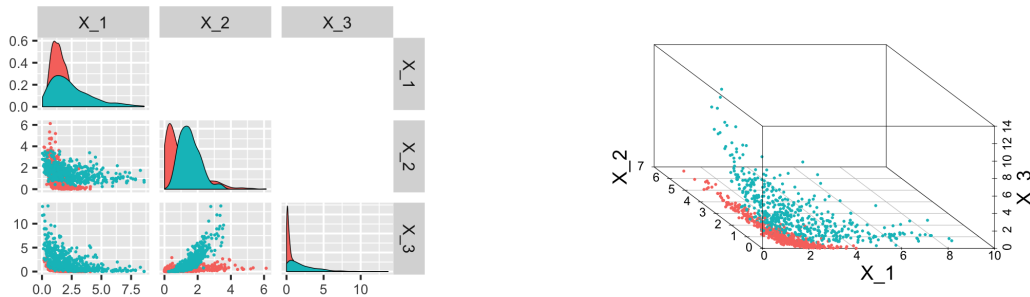


Figure 4: Pairwise (left) and 3-dimensional scatter plot (right) of simulated data (1000 observations) on x-scale under the scenario specified in Figure 3 and Table 1, where the red points show the observations of one cluster, and the green points visualize the observations of the other cluster. The diagonal of the pairwise scatter plot shows the marginal density function of each cluster's corresponding variable.

We evaluate the clustering performance of the selected algorithms by visualizing the misclassification rate and BIC value per simulation replication in box plots. For the medium sample size (1000 observations), Figure 5 shows that the vcmcc, GMM, and the mixture of multivariate t usually identify the clusters. However, the vcmcc variance on accuracy is smaller than them. The mixture of multivariate skew normal and skew-t have higher misclassification rates. Despite the high accuracy, the vcmcc and GMM have higher BIC values. However, the clustering's primary goal is to assign observations to the true clusters, and the BIC value does not always work for this goal, as discussed in Section 4 and seen here. For a clustering evaluation, lower misclassification rates can be more valuable than lower BIC values. Here 84% of the replications worked with the clustering assignment of the GMM.

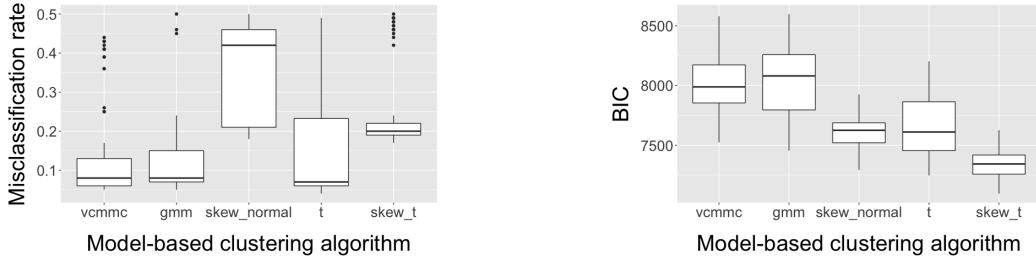


Figure 5: Comparison of the model-based clustering algorithm performances over 100 replications with 1000 observations under the scenario specified in Figure 3 and Table 1.

When the sample size is smaller (200 observations), Figure 6 shows that the vcmmc and GMM are still better algorithms than the others in terms of the misclassification rate. Their BIC values are yet higher, but they get closer to the others. Besides, the vcmmc variance on accuracy increases. 80% of the winner models in the vcmmc used the clustering assignment of the GMM as a starting partition.

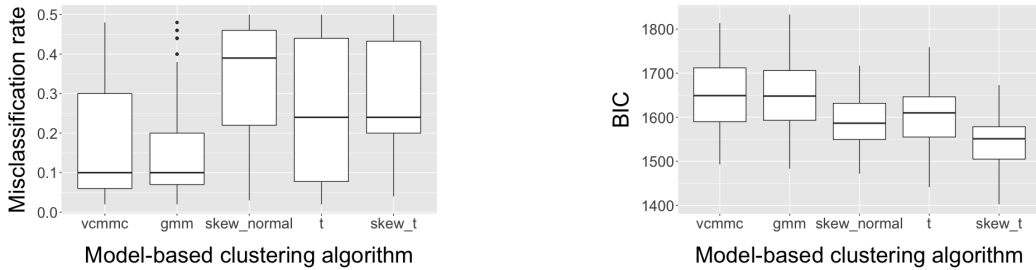


Figure 6: Comparison of the model-based clustering algorithm performances over 100 replications with 200 observations under the scenario specified in Figure 3 and Table 1.

### 5.2. The mixture of vine copulas with non-Gaussian dependencies and Gaussian/non-Gaussian margins

In this scenario, we add non-Gaussian dependencies within the clusters and simulate data on u-scale  $U_{p(1)}, U_{p(2)}$  for  $p = 1, 2, 3$  from the vine tree structures shown in Figure 7. Both clusters share the same vine tree structure and include medium sized, asymmetric tail dependencies. In contrast, the second cluster has a symmetric, non-Gaussian dependency (Frank copula) between the variables  $U_{1(2)}$  and  $U_{2(2)}$ .

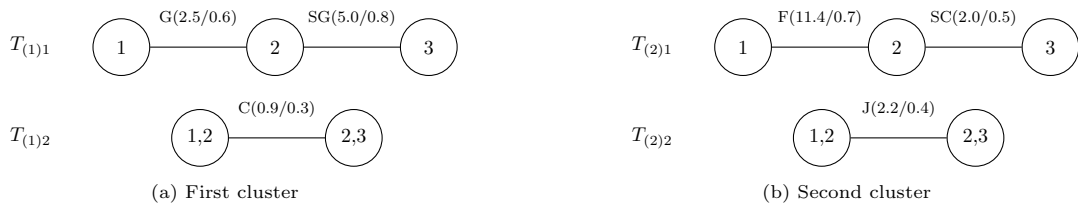


Figure 7: Vine tree structure of simulated data with two clusters. A capital letter at an edge refers to its bivariate copula family, where C: Clayton, SC: Survival Clayton, G: Gumbel, SG: Survival Gumbel, F: Frank, and J: Joe copula. The true parameter value and corresponding Kendall's  $\tau$  of the pair copula are given inside the parenthesis (parameter/Kendall's  $\tau$ ).

The next step is to obtain the data on the x-scale  $X_{p(1)}, X_{p(2)}$ , as described before. Marginal distributions and the parameters used are listed in Table 2. We illustrate simulated data (1000 observations) on the x-scale in Figure 8, where a color represents the samples from a cluster. The generated clusters are not well-separated and are non-elliptical.

|                           |                           |                           |                           |                           |                           |
|---------------------------|---------------------------|---------------------------|---------------------------|---------------------------|---------------------------|
| $F_{1(1)}(\gamma_{1(1)})$ | $F_{2(1)}(\gamma_{2(1)})$ | $F_{3(1)}(\gamma_{3(1)})$ | $F_{1(2)}(\gamma_{1(2)})$ | $F_{2(2)}(\gamma_{2(2)})$ | $F_{3(2)}(\gamma_{3(2)})$ |
| $\mathcal{N}(1, 4)$       | $Exp(0.2)$                | $Exp(0.3)$                | $\mathcal{N}(5, 4)$       | $\mathcal{N}(18, 25)$     | $Exp(0.2)$                |

Table 2: Univariate marginal distributions and associated parameters of each cluster.  $\mathcal{N}(\mu, \sigma^2)$  refers to the univariate normal distribution with mean parameter  $\mu$  and variance parameter  $\sigma^2$ ,  $Exp(\lambda)$  is defined in Table 1.

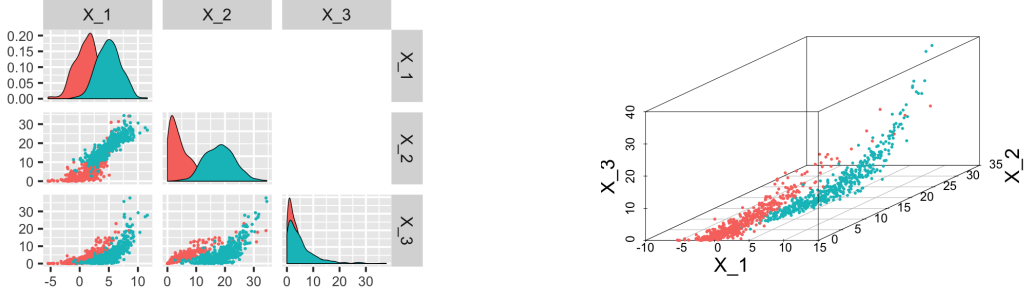


Figure 8: Pairwise (left) and 3-dimensional scatter plot (right) of simulated data (1000 observations) on x-scale under the scenario specified in Figure 7 and Table 2, where the red points show the observations of one cluster, and the green points visualize the observations of the other cluster. The diagonal of the pairwise scatter plot shows the marginal density function of each cluster's corresponding variable.

To compare the algorithms' clustering performance, Figure 9 visualizes the misclassification rate and BIC value per simulation replication in box plots for 1000 observations. The vcmmc is superior to other algorithms except for the mixtures of multivariate skew-t in terms of the misclassification rate, but it has similar results. Thus, both algorithms can partition the data very well. However, the BIC value of the vcmmc is higher. The accuracy of the vcmmc, on average, is nearly 6% higher than the GMM, and its BIC value is lower than the GMM.

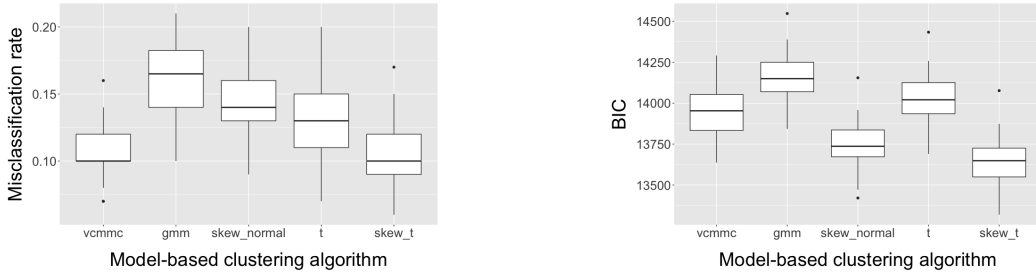


Figure 9: Comparison of the model-based clustering algorithm performances over 100 replications with 1000 observations under the scenario specified in Figure 7 and Table 2.

Figure 10 shows that the misclassification rates of the vcmmc and the mixture of multivariate skew-t do not change enormously for 200 observations, and are still lower than the others. The BIC values of all algorithms appear to be comparable.

The vcmmc usually worked with the clustering assignment of the k-means as a starting partition. 93% and 59% of the replications for the middle and small sample sizes used it. Compared to the first scenario in Section 5.1, the starting method of a winner model changed from the GMM to the k-means. It exhibits the significance of their implementation in the vcmmc. Moreover, other mixture models' clustering performances vary by a simulation scenario. The comparable models in terms of the lower misclassification rate are the vcmmc and GMM for all evaluated sample sizes in the simulation scenario given Section 5.1, where Gaussian dependencies and non-Gaussian margins within the clusters exist. However, the vcmmc and mixtures of multivariate skew-t have favorable results in this scenario with non-Gaussian dependencies and Gaussian/non-Gaussian margins within the clusters. As a result, the vcmmc shows its effectiveness and flexibility in clustering multivariate non-Gaussian data in our simulation studies.

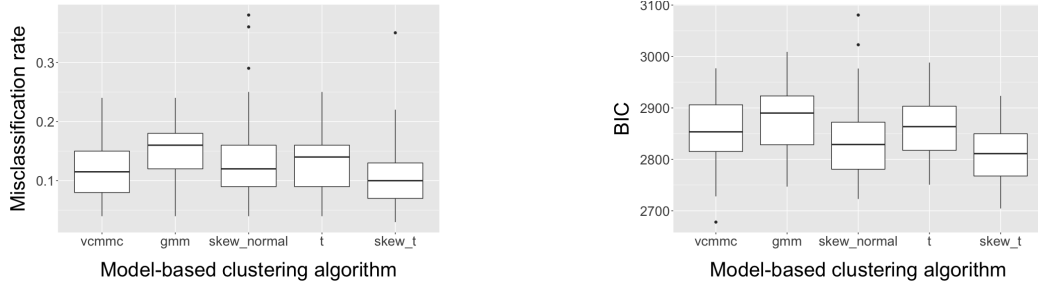


Figure 10: Comparison of the model-based clustering algorithm performances over 100 replications with 200 observations under the scenario specified in Figure 7 and Table 2.

## 6. Real data sets

In this section, we will first analyze how well the vcmmc partitions real data sets and compare the vcmmc with other models. For a fair comparison, we run other algorithms using different random seeds, thereby using different starting partitions, and report their best result in terms of the misclassification rate. Additionally, we will discuss the computational effort of the vcmmc. All computations are run on a MacBook Air (2018) with a 1,6 GHz Dual-Core Intel Core i5 and 8 GB of RAM, running R version 3.6.1. Section 6.2 will also study the influence of the truncation level of the vine tree structures on clustering performance.

### 6.1. AIS

A well-analyzed Australian Institute of Sport (AIS) data consists of 13 measurements made on 102 male and 100 female athletes. For our analysis, we select a subset of 5 variables: lean body mass (LBM), height (Ht), weight (Wt), white blood cell count (WBC), and plasma ferritins (Ferr). This sample appears to be non-Gaussian and has asymmetric patterns, as shown in Figure 11. To obtain u-data, we fit the empirical cumulative distribution function of each variable in each class. The lower panels in pairs plots show normalized contour plots, and we often do not observe Gaussian dependence. The pairwise dependence between the same pair of variables seems to be the same in both females and males, but its strength is different (e.g., LBM and Wt). Additionally, we observe that the marginal density function of WBC for both classes is similar to each other, as shown in the diagonal of the left panel in Figure 11.

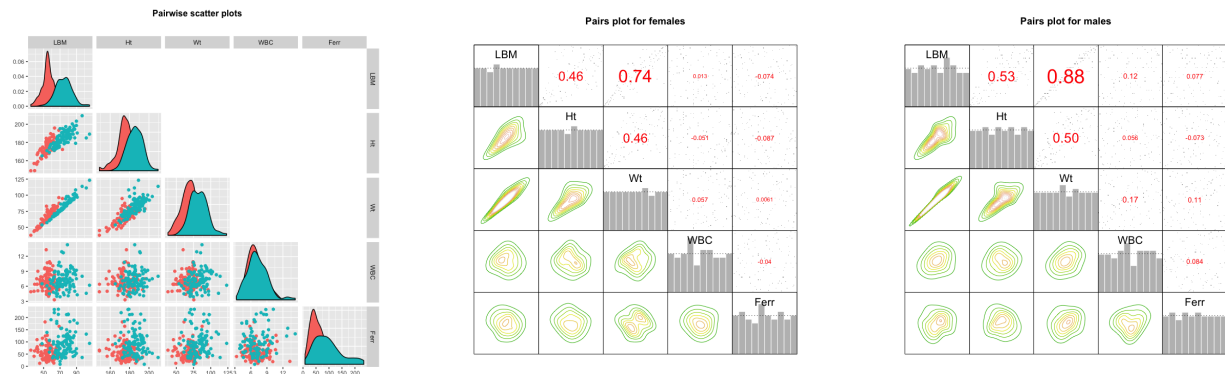


Figure 11: Pairwise scatter plot of the subset of AIS data (left), where red points for observations of females and green points for males (Diagonal: marginal density function of each class's corresponding variable). Pairs plots of females (middle) and males (right) (Upper: pairs plots of copula data, diagonal: histogram of copula margins, lower: normalized contour plots).

Since we know the gender of each observation, we can evaluate the misclassification rate of the binary classification for the clustering algorithms and associate the final clusters with the classes. Table 3 shows that the vcmmc provides a noticeably better clustering performance than the other candidates. Even though

its number of free parameters is higher than the GMM, its misclassification rate and BIC value are lower. The flexibility of the `vcmmc` to model different dependence structures and marginal densities makes the difference. Figure 12 illustrates the first tree level of the estimated vine copula models. The estimated vine tree structure is not the same for females and males. The pair of the variables `Wt` and `LBM` shows high strength and asymmetric lower tail dependence (Survival Gumbel copula) in females and males. Therefore, the dependence is especially strong for small values of `Wt` and `LBM`. A similar conclusion can be drawn for `Ht` and `LBM` in males and `Ht` and `Wt` in females (Clayton copula), but the dependency strength is medium sized. While there is a Gaussian dependency between the variables `Ht` and `Ferr` (Gaussian copula), symmetric but non-Gaussian dependency between `Wt` and `WBC` (Frank copula) exists in females and males. Appendix A presents all estimated model components and parameters by the `vcmmc`. In higher tree levels, the highest (absolute value) estimated Kendall’s  $\tau$  for females is 0.14 and exists in the second and third tree, while  $-0.22$  in the second tree for males, i.e., low strength conditional dependencies in the higher tree levels.

The `vcmmc` fits a gamma distribution for each variable in males, while a gamma distribution is selected only for `WBC` and `Ferr` in females. The `vcmmc` run 1.24 minutes, and the iterative parameter estimation step stops after two iterations. The winner model in the `vcmmc` uses the initial partition of the GMM.

| Model                     | <code>vcmmc</code> | GMM  | skew normal | t    | skew-t | k-means |
|---------------------------|--------------------|------|-------------|------|--------|---------|
| Misclassification rate    | <b>0.02</b>        | 0.09 | 0.04        | 0.29 | 0.04   | 0.34    |
| BIC                       | <b>6942</b>        | 7062 | 7055        | 7092 | 7048   | -       |
| Number of free parameters | 41                 | 30   | 51          | 41   | 51     | -       |

Table 3: Comparison of clustering algorithm performances on the subset of AIS data. The best result in each row is highlighted.

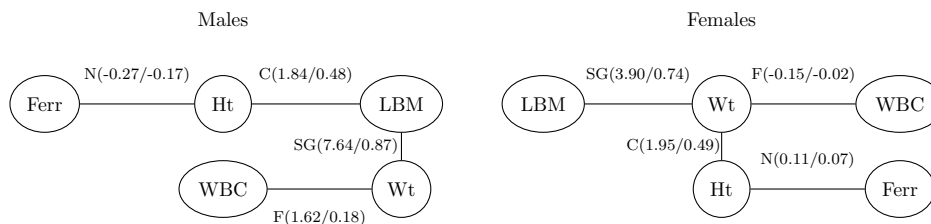


Figure 12: The first tree level of the estimated vine copula model for females and males. A capital letter at an edge refers to its bivariate copula family, where N: Gaussian, C: Clayton, SG: Survival Gumbel, and F: Frank copula. The estimated parameter value and corresponding Kendall’s  $\tau$  of the pair copula are given inside the parenthesis (estimated parameter/Kendall’s  $\tau$ ).

## 6.2. StoneFlakes

The Stone flakes data obtained from the UCI Machine Learning data repository (Dheeru & Karra Taniskidou, 2017) contains 8 variables about the inventories of 79 stone flakes. The original goal is to learn whether technological progress over a hundred thousand years can be identified by analyzing the inventory data. For our analysis, we work with the historical age determined by the archaeologists to which the samples belong and exclude them with a missing value. Thus, we use 70 observations of 3 different ages: 13 observations in Lower Palaeolithic, 23 observations in Levallois Technique, and 34 observations in Middle Palaeolithic, i.e., the actual sample size of each age is low. Because we have each observation’s age, we will evaluate the misclassification rate for the clustering algorithms and associate the final clusters with the ages.

We show pairwise scatter plots of the data and pairs plots of the ages in Figure 13, as obtained in Section 6.1. Each variable’s marginal density appears to be different for each age, and mostly non-Gaussian dependencies exist within each age. Even though diverse dependence strengths are observed in Middle Paleolithic and Lower Paleolithic, Levallois Technique mainly contains medium and low strength dependencies.

Next, we work with the different truncation levels in the `vcmmc`, i.e., modify Step V in Algorithm 1. There are 7 tree levels because the number of variables in the data set is 8. Table 4 lists the clustering results

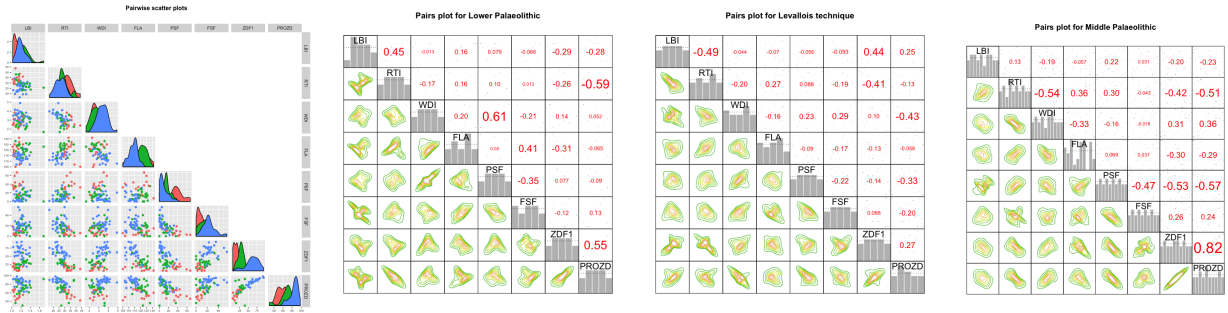


Figure 13: Pairwise scatter plots of the StoneFlakes data (left), where red points for observations of Lower Paleolithic; green points for Levallois Technique, and blue points for Middle Paleolithic (Diagonal: marginal density function of each class’s corresponding variable). Appendix B gives the variable definitions. Pairs plots of Lower Paleolithic (2nd column), Levallois Technique (3rd column), and Middle Paleolithic (right) (Upper: pairs plots of copula data, diagonal: histogram of copula margins, lower: normalized contour plots).

of different vcmmc models. We denote the truncation level inside the parenthesis in the model column, e.g.,  $\text{vcmmc}(m=1)$  refers to the vcmmc model truncated at the tree level 1. If there is no number inside the parenthesis, it corresponds to the model with a full vine specification, i.e., the vcmmc. The best model in terms of the misclassification rate and BIC value was the vcmmc truncated at the tree level 1, and it worked with the starting partition of the k-means. Even though it took more time than the  $\text{vcmmc}(m=2)$ , the number of iterative parameter estimation steps in their winner model was the same. However, the initial clustering method was different. The vcmmc with a full vine specification came after the vcmmc truncated at the tree level 1 in terms of the misclassification rate. However, its BIC value and the number of free parameters were highest, and it had the longest computation time. It also used the assignment of the k-means as an initial partition. As can be seen, the initial clustering method and misclassification rate could change depending on the truncation level. Thus, the optimal truncation level needs further studies.

| Model               | Misclassification rate | BIC         | Time elapsed (in min.) | Number of free parameters | Number of iterative parameter estimation steps | Initial clustering method utilized |
|---------------------|------------------------|-------------|------------------------|---------------------------|--|------------------------------------|
| $\text{vcmmc}(m=1)$ | <b>0.14</b>            | <b>2975</b> | 2.83                   | 71                        | 3  | k-means                            |
| $\text{vcmmc}(m=2)$ | 0.24                   | 3026        | <b>2.73</b>            | 89                        | 3  | GMM                                |
| $\text{vcmmc}(m=3)$ | 0.26                   | 3080        | 2.89                   | 104                       | 3  | GMM                                |
| vcmmc               | 0.16                   | 3232        | 2.98                   | 134                       | 3  | k-means                            |

Table 4: Clustering performance comparison of the different truncation levels in the vcmmc for StoneFlakes data. The best result in each column is highlighted. The truncation level is given inside the parenthesis in the model column.

For the comparison of the vcmmc with other clustering algorithms, Table 5 shows that the vcmmc truncated at the tree level 1 achieved the highest accuracy and lowest BIC value. The multivariate t and the vcmmc with a full vine specification followed it in terms of the misclassification rate. Even though the BIC value favored the GMM after the  $\text{vcmmc}(m=1)$ , it had the highest number of misallocations. The GMM was the most successful algorithm to find the true observations of Middle Palaeolithic, but it could not partition the remaining two groups very well. As seen in Figure 13, the observations of Middle Palaeolithic are separated from the others in most planes, but the other ages do not have such clear separation. The k-means detected the actual samples of Lower Palaeolithic because they are closer to each other in terms of the distance metric used by the k-means. For the Levallois Technique, where the dependencies are medium and low strength, the vcmmc models were the best performing algorithms with the multivariate skew-t.

Appendix B lists the estimated model components and parameters by the  $\text{vcmmc}(m=1)$ . Each cluster had a different vine tree structure. Thus, the ordering of the pair of variables for the absolute value of the estimated Kendall’s  $\tau$  value between them was not the same in each cluster. The clusters included mostly asymmetric tail dependencies with diverse dependence strengths. The highest and lowest (absolute value) estimated Kendall’s  $\tau$  value was 0.74 and 0.22 in Middle Palaeolithic, 0.50 and 0.32 in Levallois Technique,

and 0.67 and 0.39 in Lower Palaeolithic. The variables RTI and WDI in Middle Palaeolithic and LBI and RTI in Lower Palaeolithic had symmetric but non-Gaussian dependence (Frank copula). The margins of Lower and Middle Palaeolithic were mostly non-Gaussian, whereas Gaussian margins were dominant in Levallois Technique.

| Model                     | vcmmc( $m=1$ ) |             |    | vcmmc |      |    | GMM |      |    | skew normal |      |    | t  |      |    | skew-t |      |    | k-means |      |    |
|---------------------------|----------------|-------------|----|-------|------|----|-----|------|----|-------------|------|----|----|------|----|--------|------|----|---------|------|----|
|                           | 1              | 2           | 3  | 1     | 2    | 3  | 1   | 2    | 3  | 1           | 2    | 3  | 1  | 2    | 3  | 1      | 2    | 3  | 1       | 2    | 3  |
| Historical age            |                |             |    |       |      |    |     |      |    |             |      |    |    |      |    |        |      |    |         |      |    |
| Lower Paleolithic         | 10             | 3           |    | 9     | 4    |    | 6   | 7    |    | 8           | 5    |    | 12 | 1    |    | 8      | 5    |    | 13      |      |    |
| Levallois Technique       | 1              | 21          | 1  | 1     | 21   | 1  | 6   | 15   | 2  | 1           | 19   | 3  | 2  | 20   | 1  | 1      | 21   | 1  | 3       | 19   | 1  |
| Middle Paleolithic        |                | 5           | 29 |       | 5    | 29 |     | 3    | 31 |             | 4    | 30 |    | 7    | 27 |        | 5    | 29 |         | 2    | 25 |
| Misclassification rate    |                | <b>0.14</b> |    |       | 0.16 |    |     | 0.26 |    |             | 0.19 |    |    | 0.16 |    |        | 0.17 |    |         | 0.19 |    |
| BIC                       |                | <b>2975</b> |    |       | 3232 |    |     | 3028 |    |             | 3138 |    |    | 3131 |    |        | 3114 |    |         | -    |    |
| Number of free parameters |                | 71          |    |       | 134  |    |     | 76   |    |             | 158  |    |    | 134  |    |        | 158  |    |         | -    |    |

Table 5: Comparison of clustering algorithm performances on StoneFlakes data. The best result in each row is highlighted.

## 7. Conclusion

We propose a vine copula mixture model, called vcmm, that works with continuous data and fits all classes of vine tree structures. It uses parametric marginal distributions and pair copula families with a single parameter. It applies a wide range of pair copula families; thus, it accommodates diverse tail dependence and asymmetries within the clusters. Due to its parametric nature, it nicely interprets the structure of the data. Assuming the number of components in the data is known, we follow a data-driven approach for remaining model selection problems. We modify the ECM algorithm for parameter estimation. With the proposed method, we formulate a new model-based clustering algorithm, called vcmmc. The performance of the algorithm is evaluated on simulated and real data. Vine copula based clustering captures the non-Gaussian components hidden in the data better than the standard clustering methods.

To provide guidelines on a truncation level of vine tree structures to consider, we give the first analysis of its effect on clustering performance. For lower tree levels, it turns out that it impacts not only the quality of the clustering assignment but also the initial clustering method. Therefore, one possible future research direction is the modification of the proposed method to obtain parsimonious vine copula mixture models and then use it for clustering. On the one hand, the optimal truncation level can be studied, and, on the other hand, the parsimonious vine factor specification of Krupskii & Joe (2013) can be considered.

The main advantage of the vine copula based clustering is remarkable: Standard model-based clustering algorithms are often unable to capture and represent diverse characteristics of the clusters. They cannot answer whether the dependence between a pair of variables changes with the variables' different values or differs among the clusters. The vine copula based clustering, however, incorporates different dependence structures and marginal distributions. It is an appealing clustering approach since the era of big data comes with different data characteristics.

A potential drawback of the proposed method is the computational cost for high-dimensional data. This paper is an initial framework for using vine copulas with finite mixture models and clustering. Therefore, another future research direction is to handle variable selection and dimensionality reduction for vine copula based clustering. The traditional variable selection methods for other model-based clustering algorithms have to be reviewed and adjusted (e.g., Raftery & Dean (2006), Maugis et al. (2009)).

As a final future research direction, the proposed method can be extended for discrete ordinal or mixed discrete/continuous variables. The construction defined in Panagiotelis et al. (2012) and further studied in Panagiotelis et al. (2017) can be a starting point.

### Supplementary material

GitHub link for the code will follow.

## Appendix A. Estimated model components and parameters of AIS data by the vcmmc

The variable encoding is given as follows: 1: LBM, 2: Ht, 3: Wt, 4: WBC and 5: Ferr. The cluster index (1) refers to females, whereas the index (2) denotes males.

|  |   |   |  |   |                       |
|--|---|---|--|---|-----------------------|
| $\hat{F}_{1(1)}(\hat{\gamma}_{1(1)})$<br>$\mathcal{N}(55.4, 52.0)$ | $\hat{F}_{2(1)}(\hat{\gamma}_{2(1)})$<br>$\mathcal{N}(174.8, 65.0)$ | $\hat{F}_{3(1)}(\hat{\gamma}_{3(1)})$<br>$\mathcal{N}(67.5, 117.0)$ | $\hat{F}_{4(1)}(\hat{\gamma}_{4(1)})$<br>$\Gamma(17.3, 2.5)$ | $\hat{F}_{5(1)}(\hat{\gamma}_{5(1)})$<br>$\Gamma(3.83, 0.07)$ | $\hat{\pi}_1$<br>0.54 |
| $\hat{F}_{1(2)}(\hat{\gamma}_{1(2)})$<br>$\Gamma(63.0, 0.8)$       | $\hat{F}_{2(2)}(\hat{\gamma}_{2(2)})$<br>$\Gamma(623.3, 3.3)$       | $\hat{F}_{3(2)}(\hat{\gamma}_{3(2)})$<br>$\Gamma(48.1, 0.6)$        | $\hat{F}_{4(2)}(\hat{\gamma}_{4(2)})$<br>$\Gamma(15.5, 2.2)$ | $\hat{F}_{5(2)}(\hat{\gamma}_{5(2)})$<br>$\Gamma(3.4, 0.03)$  | $\hat{\pi}_2$<br>0.46 |

Table A.6: Estimated mixture weight, marginal distributions and parameters of females and males.  $\Gamma(\alpha, \beta)$  and  $\mathcal{N}(\mu, \sigma^2)$  are defined in Table 1 and Table 2, respectively.

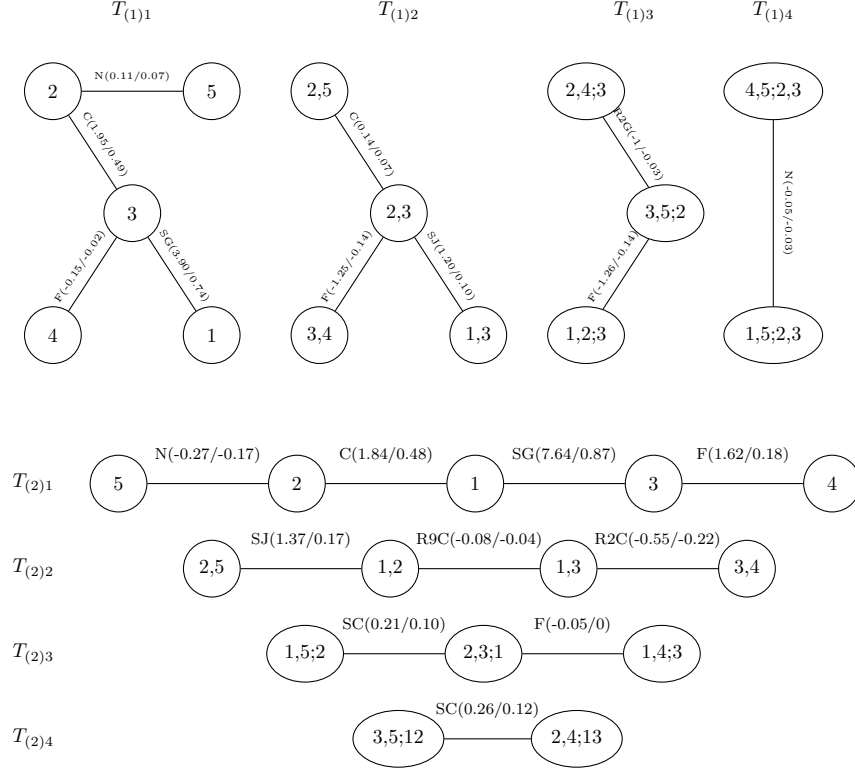


Figure A.14: Estimated vine copula models for females and males. A capital letter at an edge refers to its bivariate copula family, where N: Gaussian, C: Clayton, R9C: Rotated Clayton 90 degrees, R2C: Rotated Clayton 270 degrees, R2G: Rotated Gumbel 90 degrees, SG: Survival Gumbel, F: Frank, and SJ: Survival Joe copula. The estimated parameter value and corresponding Kendall's  $\tau$  of the pair copula are given inside the parenthesis (estimated parameter/Kendall's  $\hat{\tau}$ ).

## Appendix B. Estimated model components and parameters of StoneFlakes data by the $\text{vcmmc}(m=1)$

The variable encoding is as follows: 1: LBI (Length-breadth index of the striking platform), 2: RTI (Relative-thickness index of the striking platform), 3: WDI (Width-depth index of the striking platform), 4: FLA (Flaking angle), 5: PSF (platform primary), 6: FSF (Platform faceted), 7: ZDF1 (Dorsal surface totally worked) and 8: PROZD (Proportion of worked dorsal surface). We use the cluster index (1) for Middle Palaeolithic, (2) for Levallois Technique and (3) for Lower Palaeolithic.

|   |   |  |   |  |  |   |   |                       |
|---|---|--|---|--|--|---|---|-----------------------|
| $\hat{F}_{1(1)}(\hat{\gamma}_{1(1)})$<br>$\Gamma(205.8, 173.6)$ | $\hat{F}_{2(1)}(\hat{\gamma}_{2(1)})$<br>$\Gamma(37.1, 1.5)$  | $\hat{F}_{3(1)}(\hat{\gamma}_{3(1)})$<br>$\Gamma(46.3, 13.4)$    | $\hat{F}_{4(1)}(\hat{\gamma}_{4(1)})$<br>$\mathcal{N}(113.6, 8.8)$  | $\hat{F}_{5(1)}(\hat{\gamma}_{5(1)})$<br>$\mathcal{N}(6.6, 35.0)$  | $\hat{F}_{6(1)}(\hat{\gamma}_{6(1)})$<br>$\Gamma(5.3, 0.2)$        | $\hat{F}_{7(1)}(\hat{\gamma}_{7(1)})$<br>$\Gamma(29.5, 0.4)$        | $\hat{F}_{8(1)}(\hat{\gamma}_{8(1)})$<br>$\mathcal{N}(87.1, 29.0)$  | $\hat{\pi}_1$<br>0.43 |
| $\hat{F}_{1(2)}(\hat{\gamma}_{1(2)})$<br>$\Gamma(104.3, 83.7)$  | $\hat{F}_{2(2)}(\hat{\gamma}_{2(2)})$<br>$\Gamma(675.0, 2.6)$ | $\hat{F}_{3(2)}(\hat{\gamma}_{3(2)})$<br>$\mathcal{N}(2.7, 0.2)$ | $\hat{F}_{4(2)}(\hat{\gamma}_{4(2)})$<br>$\mathcal{N}(120.8, 20.9)$ | $\hat{F}_{5(2)}(\hat{\gamma}_{5(2)})$<br>$\mathcal{N}(17.0, 90.1)$ | $\hat{F}_{6(2)}(\hat{\gamma}_{6(2)})$<br>$\mathcal{N}(14.6, 70.2)$ | $\hat{F}_{7(2)}(\hat{\gamma}_{7(2)})$<br>$\mathcal{N}(28.0, 127.7)$ | $\hat{F}_{8(2)}(\hat{\gamma}_{8(2)})$<br>$\mathcal{N}(68.2, 144.4)$ | $\hat{\pi}_2$<br>0.41 |

| $\hat{F}_{1(3)}(\hat{\gamma}_{1(3)})$ | $\hat{F}_{2(3)}(\hat{\gamma}_{2(3)})$ | $\hat{F}_{3(3)}(\hat{\gamma}_{3(3)})$ | $\hat{F}_{4(3)}(\hat{\gamma}_{4(3)})$ | $\hat{F}_{5(3)}(\hat{\gamma}_{5(3)})$ | $\hat{F}_{6(3)}(\hat{\gamma}_{6(3)})$ | $\hat{F}_{7(3)}(\hat{\gamma}_{7(3)})$ | $\hat{F}_{8(3)}(\hat{\gamma}_{8(3)})$ | $\hat{\pi}_3$ |
|---------------------------------------|---------------------------------------|---------------------------------------|---------------------------------------|---------------------------------------|---------------------------------------|---------------------------------------|---------------------------------------|---------------|
| $\Gamma(325.4, 296.0)$                | $\Gamma(66.3, 2.0)$                   | $\Gamma(44.9, 14.6)$                  | $\mathcal{N}(118.9, 55.4)$            | $\Gamma(13.9, 0.3)$                   | $\mathcal{N}(4.9, 15.5)$              | $\Gamma(5.5, 0.3)$                    | $\mathcal{N}(54.3, 102.4)$            | 0.16          |

Table B.7: Estimated mixture weight, marginal distributions and parameters of Middle Palaeolithic, Levallois Technique and Lower Palaeolithic.  $\Gamma(\alpha, \beta)$  and  $\mathcal{N}(\mu, \sigma^2)$  are defined in Table 1 and 2, respectively.

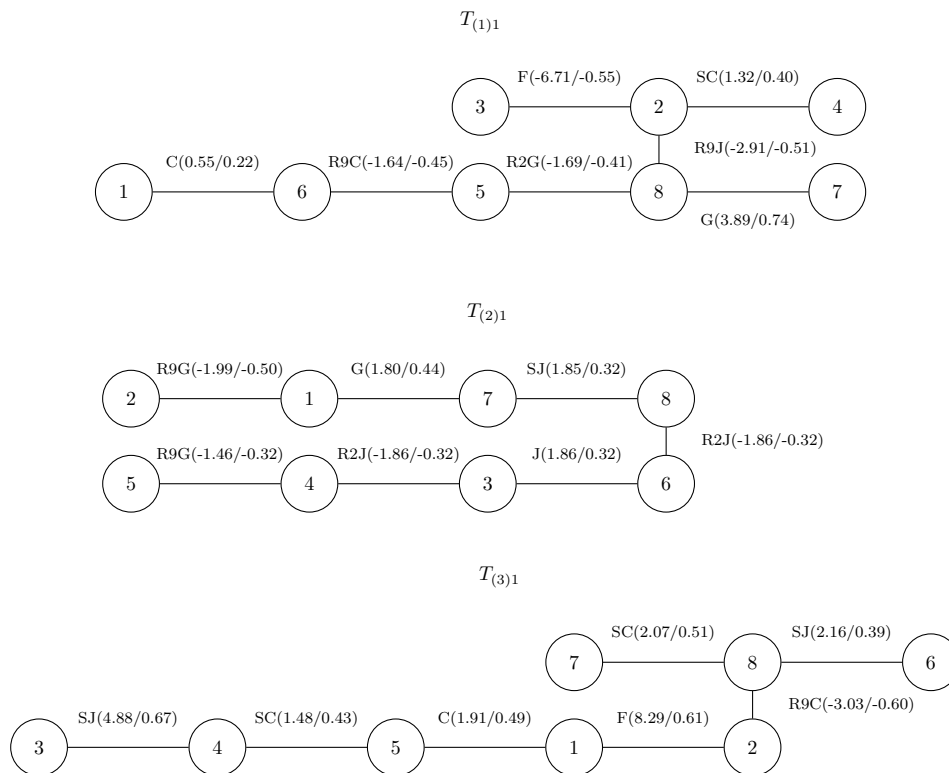


Figure B.15: The first tree level of the estimated vine copula models for Middle Palaeolithic, Levallois Technique and Lower Palaeolithic. A capital letter at an edge refers to its bivariate copula family, where C: Clayton, SC: Survival Clayton, R9C: Rotated Clayton 90 degrees, G: Gumbel, R9G: Rotated Gumbel 90 degrees, R2G: Rotated Gumbel 270 degrees, F: Frank, J: Joe, SJ: Survival Joe, R9J: Rotated Joe 90 degrees, and R2J: Rotated Joe 270 degrees copula. The estimated parameter value and corresponding Kendall's  $\tau$  of the pair copula are given inside the parenthesis (estimated parameter/Kendall's  $\hat{\tau}$ ).

## References

- Aas, K., Czado, C., Frigessi, A., & Bakken, H. (2009). Pair-copula constructions of multiple dependence. *Insurance: Mathematics and Economics*, 44, 182 – 198. doi:10.1016/j.insmatheco.2007.02.001.
- Akaike, H. (1998). Information Theory and an Extension of the Maximum Likelihood Principle. (pp. 199–213). doi:10.1007/978-1-4612-1694-0\_15.
- Andrews, J. L., & McNicholas, P. D. (2011). Mixtures of modified t-factor analyzers for model-based clustering, classification, and discriminant analysis. *Journal of Statistical Planning and Inference*, 141, 1479 – 1486. doi:10.1016/j.jspi.2010.10.014.
- Bedford, T., & Cooke, R. M. (2001). Probability density decomposition for conditionally dependent random variables modeled by vines. *Annals of Mathematics and Artificial Intelligence*, 32, 245–268. doi:10.1023/A:1016725902970.
- Bedford, T., & Cooke, R. M. (2002). Vines - A new graphical model for dependent random variables. *Annals of Statistics*, 30, 1031–1068. doi:10.1214/aos/1031689016.
- Biernacki, C., Celeux, G., & Govaert, G. (2000). Assessing a mixture model for clustering with the integrated completed likelihood. *IEEE Transactions on Pattern Analysis and Machine Intelligence*, 22, 719–725. doi:10.1109/34.865189.
- Bouveyron, C., & Brunet-Saumard, C. (2014). Model-based clustering of high-dimensional data: A review. *Computational Statistics and Data Analysis*, 71, 52–78. doi:10.1016/j.csda.2012.12.008.
- Brechmann, E. C., Czado, C., & Aas, K. (2012). Truncated regular vines in high dimensions with application to financial data. *Canadian Journal of Statistics*, 40, 68–85. doi:10.1002/cjs.10141.
- Browne, R. P., & McNicholas, P. D. (2015). A mixture of generalized hyperbolic distributions. *Canadian Journal of Statistics*, 43, 176–198. doi:10.1002/cjs.11246.

- Celeux, G., & Govaert, G. (1995). Gaussian parsimonious clustering models. *Pattern Recognition*, *28*, 781 – 793. doi:10.1016/0031-3203(94)00125-6.
- Cuvelier, E., & Fraiture, M. (2005). Clayton copula and mixture decomposition. In *Applied Stochastic Models and Data Analysis (ASMDA 2005), Brest, 17-20 May 2005*.
- Czado, C. (2019). Analyzing dependent data with vine copulas: A practical guide with R. In *Lecture Notes in Statistics*. doi:10.1007/978-3-030-13785-4\_1.
- Dang, U. J., Browne, R. P., & McNicholas, P. D. (2015). Mixtures of multivariate power exponential distributions. *Biometrics*, *71*, 1081–1089. doi:10.1111/biom.12351.
- Delignette-Muller, M. L., & Dutang, C. (2015). fitdistrplus: An R package for fitting distributions. *Journal of Statistical Software*, *64*, 1–34. URL: <http://www.jstatsoft.org/v64/i04/>.
- Dempster, A. P., Laird, N. M., & Rubin, D. B. (1977). Maximum Likelihood from Incomplete Data Via the EM Algorithm. *Journal of the Royal Statistical Society: Series B (Methodological)*, *39*, 1–38. doi:10.1111/j.2517-6161.1977.tb01600.x.
- Dheeru, D., & Karra Taniskidou, E. (2017). UCI Machine Learning Repository. URL: <http://archive.ics.uci.edu/ml>.
- Diday, E., & Vrac, M. (2005). Mixture decomposition of distributions by copulas in the symbolic data analysis framework. *Discrete Applied Mathematics*, *147*, 27 – 41. doi:10.1016/j.dam.2004.06.018.
- Dißmann, J., Brechmann, E. C., Czado, C., & Kurowicka, D. (2013). Selecting and estimating regular vine copulae and application to financial returns. *Computational Statistics and Data Analysis*, *59*, 52 – 69. doi:10.1016/j.csda.2012.08.010.
- Fraley, C., & Raftery, A. E. (1998). How Many Clusters? Which Clustering Method? Answers Via Model-Based Cluster Analysis. *The Computer Journal*, *41*, 578–588. doi:10.1093/comjnl/41.8.578.
- Franczak, B. C., Browne, R. P., & McNicholas, P. D. (2014). Mixtures of shifted asymmetric laplace distributions. *IEEE Transactions on Pattern Analysis and Machine Intelligence*, *36*, 1149–1157. doi:10.1109/TPAMI.2013.216.
- Hennig, C. (2010). Methods for merging Gaussian mixture components. *Advances in Data Analysis and Classification*, *4*, 3–34. doi:10.1007/s11634-010-0058-3.
- Joe, H. (1996). Families of  $m$ -variate distributions with given margins and  $m(m-1)/2$  bivariate dependence parameters. In *Distributions with fixed marginals and related topics* (pp. 120–141). Institute of Mathematical Statistics. doi:10.1214/lnms/1215452614.
- Joe, H. (2014). *Dependence Modeling with Copulas*. New York: Chapman and Hall/CRC. doi:10.1201/b17116.
- Joe, H., & Xu, J. J. (1996). The Estimation Method of Inference Functions for Margins for Multivariate Models. *Technical Report no. 166, Department of Statistics, University of British Columbia*, (pp. 1–21). doi:10.14288/1.0225985.
- Karlis, D., & Xekalaki, E. (2003). Choosing initial values for the EM algorithm for finite mixtures. *Computational Statistics and Data Analysis*, *41*, 577 – 590. doi:10.1016/S0167-9473(02)00177-9.
- Kim, J. M., Kim, D., Liao, S. M., & Jung, Y. S. (2013). Mixture of D-vine copulas for modeling dependence. *Computational Statistics and Data Analysis*, *64*, 1–19. doi:10.1016/j.csda.2013.02.018.
- Kosmidis, I., & Karlis, D. (2016). Model-based clustering using copulas with applications. *Statistics and Computing*, *26*, 1079–1099. doi:10.1007/s11222-015-9590-5.
- Krupskii, P., & Joe, H. (2013). Factor copula models for multivariate data. *Journal of Multivariate Analysis*, *120*, 85 – 101. doi:10.1016/j.jmva.2013.05.001.
- Lee, S., & McLachlan, G. J. (2014). Finite mixtures of multivariate skew t-distributions: Some recent and new results. *Statistics and Computing*, *24*, 181–202. doi:10.1007/s11222-012-9362-4.
- Lin, T. I., Lee, J. C., & Yen, S. Y. (2007). Finite mixture modelling using the skew normal distribution. *Statistica Sinica*, *17*, 909–927. URL: <http://www.jstor.org/stable/24307705>.
- Maugis, C., Celeux, G., & Martin-Magniette, M. L. (2009). Variable selection for clustering with gaussian mixture models. *Biometrics*, *65*, 701–709. doi:10.1111/j.1541-0420.2008.01160.x.
- McLachlan, G. J., & Peel, D. (2000). *Finite mixture models/Geoffrey McLachlan, David Peel*. Wiley New York; Chichester. doi:10.1002/0471721182.
- McNicholas, P. D. (2016). Model-Based Clustering. *Journal of Classification*, *33*, 331–373. doi:10.1007/s00357-016-9211-9.
- Meng, X.-L., & Rubin, D. B. (1993). Maximum Likelihood Estimation via the ECM Algorithm: A General Framework. *Biometrika*, *80*, 267–278. doi:10.2307/2337198.
- Morales-Nápoles, O. (2010). Counting vines. In *Dependence Modeling: Vine Copula Handbook*. doi:10.1142/9789814299886\_0009.
- Nagler, T., Schepsmeier, U., Stoeber, J., Brechmann, E. C., Graeler, B., & Erhardt, T. (2019). *VineCopula: Statistical Inference of Vine Copulas*. URL: <https://CRAN.R-project.org/package=VineCopula>.
- Panagiotelis, A., Czado, C., & Joe, H. (2012). Pair copula constructions for multivariate Discrete Data. *Journal of the American Statistical Association*, *107*, 1063–1072. doi:10.1080/01621459.2012.682850.
- Panagiotelis, A., Czado, C., Joe, H., & Stöber, J. (2017). Model selection for discrete regular vine copulas. *Computational Statistics and Data Analysis*, *106*, 138 – 152. doi:10.1016/j.csda.2016.09.007.
- Peel, D., & McLachlan, G. J. (2000). Robust mixture modelling using the t distribution. *Statistics and Computing*, *10*, 339–348. doi:10.1023/A:1008981510081.
- Prates, M. O., Cabral, C. R. B., & Lachos, V. H. (2013). mixsmn: Fitting finite mixture of scale mixture of skew-normal distributions. *Journal of Statistical Software*, *54*, 1–20. URL: <http://www.jstatsoft.org/v54/i12/>.
- Punzo, A., & McNicholas, P. D. (2016). Parsimonious mixtures of multivariate contaminated normal distributions. *Biometrical Journal*, *58*, 1506–1537. doi:10.1002/bimj.201500144.
- R Core Team (2019). *R: A Language and Environment for Statistical Computing*. R Foundation for Statistical Computing Vienna, Austria. URL: <https://www.R-project.org/>.
- Raftery, A. E., & Dean, N. (2006). Variable selection for model-based clustering. *Journal of the American Statistical Association*

- ation, 101, 168–178. doi:[10.1198/016214506000000113](https://doi.org/10.1198/016214506000000113).
- Schwarz, G. (1978). Estimating the Dimension of a Model. *The Annals of Statistics*, 6, 461–464. doi:[10.1214/aos/1176344136](https://doi.org/10.1214/aos/1176344136).
- Scrucca, L., Fop, M., Murphy, T. B., & Raftery, A. E. (2016). Mclust 5: Clustering, classification and density estimation using Gaussian finite mixture models. *R Journal*, 8, 289–317. doi:[10.32614/rj-2016-021](https://doi.org/10.32614/rj-2016-021).
- Sklar, A. (1959). Fonctions de Répartition à n Dimensions et Leurs Marges. *Publications de L'Institut de Statistique de L'Université de Paris*, (pp. 229–231).
- Stöber, J., Joe, H., & Czado, C. (2013). Simplified pair copula constructions-Limitations and extensions. *Journal of Multivariate Analysis*, 119, 101 – 118. doi:[10.1016/j.jmva.2013.04.014](https://doi.org/10.1016/j.jmva.2013.04.014).
- Sun, M., Konstantelos, I., & Strbac, G. (2017). C-Vine Copula Mixture Model for Clustering of Residential Electrical Load Pattern Data. *IEEE Transactions on Power Systems*, 32, 2382–2393. doi:[10.1109/TPWRS.2016.2614366](https://doi.org/10.1109/TPWRS.2016.2614366).
- Vrac, M., Chédin, A., & Diday, E. (2005). Clustering a global field of atmospheric profiles by mixture decomposition of copulas. *Journal of Atmospheric and Oceanic Technology*, 22, 1445–1459. doi:[10.1175/JTECH1795.1](https://doi.org/10.1175/JTECH1795.1).